Adriana Maria Teles Sampaio

Bachelor Degree in Chemical and Biochemical Engineering

Biogas production and purification using membrane processes

Dissertation to obtain Master Degree in Chemical and Biochemical Engineering

Supervisor: Doutora Luísa A. Neves, Investigadora Auxiliar, FCT-UNL

Co-supervisor: Doutora Mónica Carvalheira, Investigadora, FCT-UNL

Jury:

President: Professor Doutor Mário Fernando José Eusébio

Supervisor: Doutora Luísa Alexandra Neves

FACULDADE DE CIÊNCIAS E TECNOLOGIA
UNIVERSIDADE NOVA DE LISBOA

September 2019

Adriana Maria Teles Sampaio

Bachelor Degree in Chemical and Biochemical Engineering

Biogas production and purification using membrane processes

Dissertation to obtain Master Degree in Chemical and Biochemical Engineering

Supervisor: Doutora Luísa A. Neves, Investigadora Auxiliar, FCT-UNL

Co-supervisor: Doutora Mónica Carvalheira, Investigadora, FCT-UNL

Jury:

President: Professor Doutor Mário Fernando José Eusébio

Supervisor: Doutora Luísa Alexandra Neves

Faculty of Sciences and Technology

NOVA University of Lisbon

September 2019

Biogas production and purification using membrane processes

Agradecimentos

Finalmente chega ao fim uma das experiências mais importantes e enriquecedoras da minha vida e não poderia deixar de agradecer a todos aqueles que sempre me apoiaram incondicionalmente, que me deram força para continuar e que nunca me deixaram baixar os braços.

Gostaria de agradecer às minhas orientadoras, Luísa Neves e Mónica Carvalheira pela oportunidade de me integrar em dois grupos, BIOENG e LMPgroup e de poder aprender um pouco do mundo de membranas e de bioengenharia.

Um agradecimento muito especial ao Bruno Oliveira, que me acompanhou no laboratório de BIOENG desde o primeiro dia e que foi das pessoas que mais coisas me ensinou durante a realização desta tese.

Gostaria também de agradecer às pessoas integrantes do grupo de LMP que tive a oportunidade de conhecer e de conviver diariamente. Agradeço à Rita Nabais, por todo o tempo que passou comigo no laboratório no início desta tese, por tudo o que me ensionou e pela paciência que teve em me explicar muitas das coisas que sei de membranas. À Rosa Nascimento quero muito agradecer pela ajuda e pela boa disposição que diariamente me transmitiu.

À doutora Claudia Pereira queria agradecer a disponibilidade, simpatia e ajuda que me deu na síntese e caracterização do MOF.

A todos os meus amigos que me apoiaram durante estes anos, Rita Freitas, Diogo Boto, Beatriz Nobre e Tiago Ferreira mesmo não estando presentes diariamente sei que sempre me apoiaram e torceram por mim. Às minhas melhores amigas, Marta Bexiga, Carolina Cravalho, Sara Coutinho e Carolina Marques nem sei como agradecer todo o apoio e força que me deram, sem elas teria sido impossível! À Ana Patrícia quero muito agradecer por me ter encorajado a continuar e a enfrentar todos os obstáculos que surgiram ao longo destes meses.

Ao meu namorado, André Santos, quero agradecer todo o carinho, amor e paciência que teve comigo, a amizade sem fim, as manhãs, tardes e noites que teve ao meu lado.

À tia Carla e tio Vivi quero agradecer todo o carinho e apoio que me deram.

Por fim, quero agradecer aos meus pais, sem eles nada disto seria possível. Obrigada por me terem proporcionado a maior experiência da minha vida, por terem acreditado que seria capaz e por terem investido no meu futuro! Ao meu irmão que sempre me deu força para não desistir e que está, até hoje, à espera de um jantar pago com o meu primeiro ordenado. Às minhas primas Bárbara, Amora e Benedita e à minha tia Isabel quero agradecer por terem sempre acreditado em mim, por todas as velinhas que acenderam e por todas as palavras de coragem que me deram. Aos meus avós, Manuel Trindade e Maria de Matos por todo o carinho e amor que me deram desde sempre. E por último quero muito agradecer aos meus dois anjinhos, Avó Perpétua e Avô Horácio que mesmo não estando presentes fisicamente estiveram e estarão sempre a olhar por mim!

A todos, um grande obrigado

Abstract

In this master thesis, a single-stage anaerobic co-digestion system was operated treating a mixture of leachate and tannery wastewater, increasing salinity from 5 to 15 g Na^+ L^{-1}.

Biogas production (1.6 ± 0.3 – 3.0 ± 0.3 L d^{-1}) increased as salinity increased up to 10 g Na^+ L^{-1} as well as CH_4 yield (0.29 ± 0.03 – 0.33 ± 0.03 L CH_4 g^{-1} COD). At 15 g Na^+ L^{-1}, a decrease in biogas production and granules fragmentation were observed. Overall, the results showed that the microbial community was able to withstand salinities up to 15 g Na^+ L^{-1}, presenting a good performance on the co-treatment of leachate and tannery wastewater.

The second part of this master thesis was focused on the effect of combining metal organic frameworks (MOF-5), with high adsorption properties towards CO_2 when compared with CH_4, with a combination of different poly(ionic liquid)/ionic liquid (PIL/IL) membranes for biogas upgrading. The MOF-5 was incorporated at different loadings (10, 20 and 30 wt%), and mixed matrix membranes (MMMs) were prepared by solvent evaporation method. The results showed that MOF-5 particles were uniformly dispersed into the PIL/IL matrix, except for PIL $C(CN)_3$/40 [C_2MIM][$C(CN)_3$]. The prepared PIL/IL/MOF-5 membranes revealed suitable thermal stability (T_{onset} up to 300-380ºC) for biogas upgrading, but a loss of mechanical stability was found after the incorporation of MOF-5. Nevertheless, increasing MOF-5 content in the MMMs resulted in an improvement on CO_2 permeability, which increased 133% for PIL Tf_2N/40 [C_2MIM][BETi]/30 MOF-5 when compared to PIL Tf_2N/40 [C_2MIM][BETi]. It was therefore possible to demonstrate the improvement of CO_2/CH_4 separation performance of this MMMs system using MOF-5, which opens the perspective of using these materials for biogas upgrading.

Keywords: single-stage anaerobic co-digestion system; biogas; salinity; biogas upgrading; mixed matrix membranes; metal organic frameworks;

Resumo

Nesta dissertação foi desenvolvido um sistema de co-digestão anaeróbia de uma fase por forma a tratar uma mistura de lixiviados e curtumes através do aumento da salinidade de 5 a 15 g Na^+ L^{-1}. A produção de (1.6 ± 0.3 – 3.0 ± 0.3 L d^{-1}) aumentou com o aumento da salinidade até 10 g Na+ L-1, bem como o rendimento de metano (CH_4) (0.29 ± 0.03 – 0.33 ± 0.03 L CH_4 g^{-1} COD). A 15 g Na^+ L^{-1}, foi observada uma diminuição da produção de biogás bem como a fragmentação dos grânulos. No geral, os resultados mostraram que a comunidade microbiana foi capaz de suportar salinidades de até 15 g Na^+ L^{-1}, apresentando um bom desempenho no co-tratamento de lixiviados e curtumes.

A segunda parte desta dissertação focou-se no efeito da combinação de redes (*metal-organic frameworks)* (MOF-5), com elevadas propriedades de adsorção em relação do CO_2 quando comparado com o CH_4, com diferentes membranas constituídas por líquidos iónicos poliméricos/líquidos iónicos (PIL/IL) para a purificação do biogás. Após a incorporação de diferentes concentrações de MOF-5 (10, 20 e 30 p/p%), as membranas de matriz mista (MMMs) foram preparadas pelo método de evaporação de solvente. Os resultados mostram que as partículas de MOF-5 foram uniformemente dispersas na matriz PIL/IL, exceto para a membrana PIL $C(CN)_3$/40 $[C_2MIM][C(CN)_3]$. As membranas PIL/IL/MOF-5 preparadas revelaram uma estabilidade térmica adequada (T_{onset} entre 300-380 ºC) para a purificação do biogás, apesar da perda de estabilidade térmica após a incorporação de MOF-5. No entanto, o aumento da quantidade de MOF-5 nas MMMs resultou numa melhoria na permeabilidade do CO_2, que aumentou 133% para a PIL Tf_2N/40 $[C_2MIM][BETi]$/30%MOF-5 quando comparada à PIL/IL. Desta forma, foi possível melhorar o desempenho da separação de CO_2/CH_4 deste sistema de MMMs através da utilização de MOF-5, o que permite a sua utilização para a purificação do biogás.

Palavras chave: Sistema de co-digestão anaeróbia de uma fase; biogás; salinidade; purificação do biogás; membranas de matriz mista; metal-organic frameworks

List of contents

List of figures

List of tables

List of Abbreviations

AD	Anaerobic digestion
COD	Chemical oxygen demand
CSP	Chemical scrubbing process
CSTR	Continuous stirred-tank reactor
DEA	Diethanolamine
DMF	Dimethylformamide
EGSB	Expanded granular sludge bed
FTIR	Fourier Tranform Infrared Spectroscopy
GC	Gas chromatography
HAc	Acetic acid
HBut	Butyric acid
HIsoB	Isobutiric acid
HIsoV	Isovaleric acid
HPr	Propionic acid
HPWS	High pressure water scrubbing
HRT	Hydraulic retention time
HVal	Valeric acid
IL	Ionic liquid
MDEA	Methyldiethanolamine
MEA	Monoethanolamine
MMM	Mixed matrix membrane
MOF	Metal organic framework
OA	Organic acid
OLR	Organic loading rate
OPS	Organic physical scrubbing
PIL	Poly(ionic liquid)
PSA	Pressure swing adsorption
PZ	Piperazine
SCOD	Soluble chemical oxygen demand
SEM	Scanning Electron Microscopy
TGA	Thermogravimetric analysis
TSS	Total suspended solids
UASB	Upflow anaerobic sludge blanket
VFA	Volatile fatty acid

VSS	Volatile suspended solids
Cations	
[C_2MIM]	1-ethyl-3-methylimidazolium
[C_4MIM]	1-butyl-3-methylimidazolium
Polycation	
[py_{11}]	Poly(diallyldimethylammonium
Anions	
[Tf_2N]	Bis(trifluoromethylsulfonyl)imide
[BETi]	Bis(pentafluoroethylsulfonyl)imide
[$C(CN)_3$)]	Tricyanomethanide
[PF_6]	Hexafluorophosphate

List of variables

A	Membrane area
l	Membrane thickness
P	Permeability
p	Pressure
p_{feed}	Pressure in feed compartment
p_{perm}	Pressure in the permeate compartment
Q	Flow rate
t	Time
T_{dec}	Decomposition temperature
T_{onset}	Onset temperature
V_{feed}	Volume of the feed compartment
V_{perm}	Volume of the permate compartment
α	Ideal selectivity
β	Geometric parameter

1. Introduction

1.1. Problem statement

Nowadays, the increase of the industrialization, as a consequence of economic growth, resulted in the generation of a huge quantity of wastes from several sources such as municipal, industrial and agricultural.[1] Usually, these wastes and other solid wastes are disposed and treated using conventional treatment methods, where landfill is one of the most and widely technology used.[2]

In landfills, where are mainly collected municipal wastes, occurs the decomposition of organic matter resulting in a wastewater known as leachate and gases that contributes to 20% of the global methane emissons.[3] Leachate from landfills contain typicaly both simple and complex components, such as, high organic matter content, salts and ammonia and their accumulation in environment is a huge problem since causes several pollution problems, namely contamination of soil, surface and groundwater.[4–6] Despite these disadvantages, landfills still remains the most used alternative to dispose wastes.[7]

Some industries, such as seafood, petroleum and leather industries, produce saline effluents with high organic content and high amounts of salt.[4,8] Leather industries involves the addition of salt in the tanning process that occurs through several steps and where raw hides and skins are transformed in finished leather products. The tanning process involves high quantities of water in each step, producing hypersaline streams, such as pickling wastewater, and the soak liquor generated by the soaking of hides and skins containing, sometimes, about 80g L^{-1} of NaCl.[4] The discharge of these type of effluents in the environment without pre-treatment leads to the contamination of agriculture fields, water potability and aqualife. The use of physico-chemical methods to treat saline effluents is the alternative currently used; however presents several disadvantages, namely high energy consumption and high running costs. Another alternatives are discharge saline effluents to the seaside, that is not feasible, and desalination by reverse osmosis, that is very expensive.[9] In the last 10 years the interest in wastewaters with high sanility has been increasing due to the dimension of this problem.[4] Biological processes are developed as an alternative but the high salinity of this type of wastes effect negatively the process.

Taking into account the problems associated with current treatment strategies, the development of economic and environmental treatment technologies is crucial.

In this context, the present linear economic model of "*take-make-consume-dispose*" is being slowly substitute by circular economy, with a sustainable approach focused in maintain and retain the value of materials and products.[10] Therefore, the treatment of wastes and wastewater with resources recovery through an integrated system offers an economic and versatile way for a global sustainable development. Examples of these systems include the production of biopolymers and biogas from anaerobic digestion.[11]

Anaerobic digestion (AD) has been studied in recent years as a suitable technology and an energy-efficient process for biological waste treatment with high benefits, such as waste reduction and biogas

production.[12] Therefore, AD is reviewed as a promising sustainable solution that will not only reduce the negative impacts of wastes accumulation, mentioned above, but also generate an alternative to the current increase of fossil fuels consumption, producing methane-rich biogas, which can be used as a renewable source of energy. The production of biogas through anaerobic digestion was considered as one of the most efficient and environmental beneficial technology for bioenergy production.[13] However, several factors such as, organic carbon, nutrients and mineral contents, can affect the AD efficiency. One option to improve the efficiency of the process is the co-digestion where a combination of several wastes with complementary characteristics are treated.[14]

The present study was focused on the development of a new membrane for biogas purification produced through a co-digestion of two type of wastewaters, tannery and leachate, using the AD process at laboratory scale .

1.2. Anaerobic digestion process

Anaerobic digestion (AD) is a multistep biological process where oxygen is absent. In AD, biogas is produced through the conversion of organic matter by a consortium of anaerobic microorganisms under managed conditions. This process can occur naturally in environments where organic material and low redox potencial are available, such as sediments of lakes and ditches, municipal landfills or municipal sewers.[15] Several types of wastes can be used for biogas production using anaerobic reactors (**Figure 1.1**).

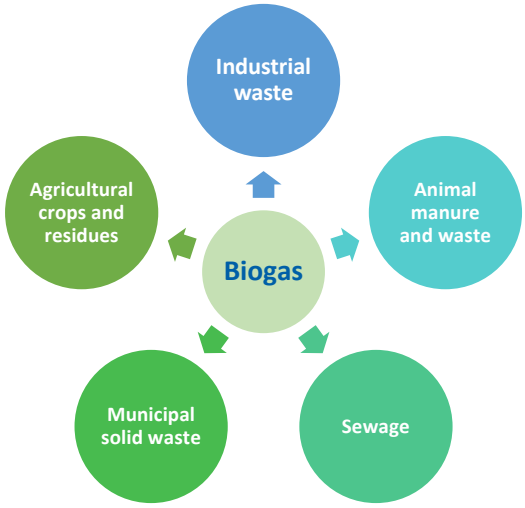

Figure 1. 1. Examples of wastes which can be anaerobically digested to produce biogas (Adapted from Abbasi et al. (2012) [16])

The biogas produced through AD processes is mostly composed of about 55-70% of methane (CH_4) and 30-45% carbon dioxide (CO_2) and trace amounts of another substances such as nitrogen (N_2), hydrogen sulfide (H_2S) and ammonia (NH_3) (**Table 1.1**).

Table 1. 1. Typical composition of biogas (Adapted from Bothi (2007)[17])

Component	Units	Content
CH_4	Vol%	55-70%
CO_2	Vol%	30-45%
N_2	Vol%	0-2%
H_2S	Vol%	>0.05
NH_3	Vol%	~0.01

1.2.1. Microbiological aspects and main pathways of anaerobic digestion

The production of biogas in AD processes is composed by four distinct steps, namely: Hydrolysis, acidogenesis, acetogenesis and methanogenesis **(Figure 1.2**). During these four steps, biochemical reactions governed by the microbial community in AD reactor takes place.

Hydrolysis

Hydrolysis is the first step of anaerobic digestion process where the polymeric particles are degraded through the action of exo-enzymes, which are secreted by hydrolytic bacteria to produced soluble molecules that can be used by acidogens. Thus carbohydrates, proteins and fats are converted into sugar, amino acids and fatty acids, respectively.[2] Despite of this, it is relevant to know that hydrolysis is a relatively slow step due to the slow degradation of certain substances, such as lignin and cellulose, which can limit the rate of the process.[19]

Acidogenesis

The soluble molecules formed during hydrolysis are further absorbed by acidogenic bacteria that are able to convert them into various organic acids such as propionate and butyrate, as well as H_2, CO_2 and alcohols.[20] Acidogenesis is the most faster step in the anaerobic digestion since acidogenic bacteria has ten to twentyfold higher bacterial growth rates and fivefold higher bacterial yield and conversion rates compared with methanogens.[15] Acidogens also tolerate extreme conditions such as high temperature, low pH and high organic loading rate (OLRs).[21]

Acetogenesis

Acetogenesis is the third step of anaerobic digestion. In this step, the organic acids and alcohols produced through acidogens are converted largely into acetate, as well as, H_2 and CO_2 by the acetogens and used by the methanogens later.[22] In most cases H_2 is not detected due to the relationship between acidogens (H_2 producers) and methanogens (H_2 consumers), also known as syntrophic interaction. This interaction allows to maintain a low H_2 partial pressure.[21]

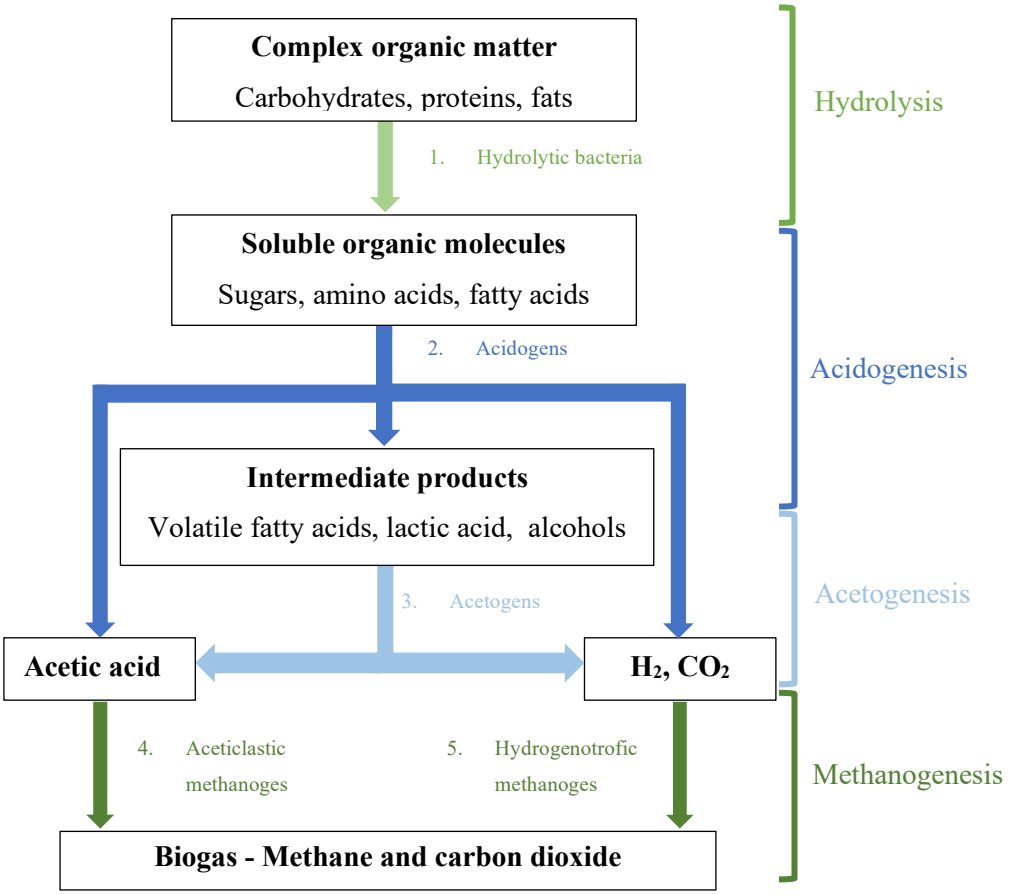

Figure 1. 2. Stages of anaerobic digestion process and the different bacterial group involved (Adapted from Lier et al. (2008) and Costa et al (2015) [15,18])

Methanogenesis

The fourth and last step of anaerobic digestion is methanogenesis. During this step, hydrogenotrophic and aceticlastic methanogens are the two groups of methanogenic archaea responsibles to produce CH_4, CO_2, H_2 and other residual gases. Hydrogenotrophic methanogens are responsibles to produced CH_4 using H_2 and CO_2, while aceticlastic methanogens convert acetate into CH_4.[15] The production of CO_2 is higher from hydrogenotrophic methanogens (70% of the total CO_2 produced) when compared to aceticlastic methanogens (30% of the total CO_2 produced).[23]

1.2.2. Single-Stage anaerobic digestion system

In AD processes for biogas production, a single-stage system is conventionally used where the hydrolysis, acidogenesis, acetogenesis and methanogenesis occur in the same reactor.[24,25] The lower capital and operating costs, as well as, low sludge production make this type of process attractive, mainly for bigger plants.[26] However, the microorganisms of acidogenesis and methanogenesis have distinct sensitivity to environmental conditions, physiology and growth kinetics.[27] Thus, the operational

conditions are carefully maintained in order to ensure the survival of all microorganisms, namely the methanogens that are more vulnerable than acidogens.

1.2.3. Operational and environmental conditions

In AD several factors, such as reactor configuration, mixing strategy and biomass growth rate, are essencial to achieve a good performance in terms of organic matter conversion and biogas production. Furthermore, it is also essential to controll environmental conditions, such as pH, nutrients content, hydraulic loading rate (HRT) and OLR, in order to allow a good stability since microorganisms, specially methanogens, are very susceptible to environmental changes.[22]

Reactor configuration

In biogas production process is important to ensure the retention of the biomass sludge in the reactor in order to avoid biomass washout. Therefore, AD can be divided into "low rate" and "high rate" systems and each one is used to treat different wastes depending on their organic loadings. Low rate systems, which are operated with long HRTs, include batch reactor and continuous stirred tank reactor (CSTR) and are generally used to treat slurries and solid wastes. High rate systems use shorter HRTs and are mainly used for wastewater treatment. Examples of this type of system include anaerobic filter, expanded granular sludge bed (EGSB) and Upflow anaerobic sludge blanket (UASB).[28]

Anaerobic granular biomass

Anaerobic granular biomass possess some very specific properties, such as high sedimentation velocity and high methanogenic activity, which make it very suitable when the process is applied in an UASB (Upflow Anaerobic Sludge Blanket) reactor.[29] In these processes granules incorporate microorganisms and are suspended in liquid containing dissolved organic material.[22] Therefore the microrganisms are more protected to adverse conditions, such as high salinities.

Temperature

Operating temperature is one of the most significant parameters influencing bioreactors performance.[5] Effluent quality, CH_4 yield, effluent quality and enzimes activity are parameters influenced by temperature and abrupt changes may cause disturbance, mainly for methanogens.[30]

There are two main temperature ranges of operation and different microorganisms operate in each range. Mesophilic microorganisms has an optimum temperature between 30-40°C and thermophilic microorganisms are most productive in the 50-60°C range.[31] In thermophilic operations slight variations, as 1 ºC day^{-1}, can lead to process failure.[5] In the other hand, under mesophilic operation, changes of about 3 ºC day^{-1} have no impact in CH_4 production.[13] Therefore, bioreactors usually operate in mesophilic temperatures.

Salinity

As mentioned above, salinity can effect negatively the biogas production performance since the presence of sodium in effluent inhibites waste biodegradation and in cases where granules are used can lead to their disintegration.[32] For these reasons is necessary control the wastewater salinity content in order to promote the adaptation of the microbial community .

pH and redox potencial

The growth rate of methanogens and acidogens are mostly affected by pH and each one has a different optimum pH range. For a single-stage configuration, the reactor is typically maintained between methanogenic limits (neutral pH (6.5 - 7.2)) since methanogenesis is considered a rate-limiting step and methanogens are more sensitive than acidogens to pH changes.[30] In these conditions is possible to prevent the predominance of acidogens. The pH can decrease (< 6.0) or increase (> 8.0) due to Volatile Fatty Acids (VFA) accumulation or ammonia accumulation, respectively.[13]

The redox potential is an important parameter that must be controlled in an anaerobic process. Methanogens need a low redox potential around -300 mV for the optimum performance.[22]

Organic Loading Rate and Hydraulic Retention Time

Hydraulic retention time (HRT) is one of the most important parameter that affects the reactor operation and needs to be optimized in order to allow a higher degradation of the organic matter. This optimization depends on process conditions and feedstock composition, namely reactor volume (V) and influent flow rate (Q) and can be defined by the equation HRT=V/Q.[33]

The control of organic loading rate (OLR) is crucial to achieve stability in anaerobic processes and depends of HRT and chemical oxygen demand (COD).[34] OLR corresponds to the quantity of organic matter fed per reactor volume per unit time and can be also expressed in terms of COD concentration ($Kg_{COD}\ L^{-1}\ d^{-1}$). In single stage systems, instability in OLR can negatively affect the balance between acidogenesis and methanogenesis. Acidogens can operate at high loading rates and, consequently, produce high amounts of VFAs that methanogens may not be able to consume due to their slower growth rates which can leads to reactor acidification.[35]

Nutrients

The nutrients are one of the factors that effects the growth and activity of microorganisms and consequently biogas production. The lack of essential nutrients can also develop problems such as acidification, process instability and low methane yield. Nutrients can be divided in two categories, micronutrients such as calcium and magnesium and macronutrients like nitrogen and phosphorus.[36]

1.3. Biogas Upgrading

As previously mentioned, the biogas produced through AD processes can be optimized and used as a renewable source of energy. Like natural gas, biogas can be a fuel for a large number of applications. Some of these applications are production of heat and steam, electricity generenation and as a vehicle fuel.[30] Depending on the end use, biogas may need to be cleaned and purified before utilization, removing the impurities such as H_2S, N_2 and NH_3 and upgrade decreasing their CO_2 content.[37] Some applications, such as vehicle fuel and grid injection, require a high energy content in the gas, which is in direct proportion to the CH_4 concentration. Through upgrading technologies is possible to remove CO_2 and increase the energy content of the gas.[38]

1.3.1. Technologies for biogas upgrading

Biogas upgrading corresponds to the removal of CO_2 from the biogas and consequently the increase of CH_4 content which should be more than 95%.[13] Therefore to select the upgrading technology it is necessary to take account various factors, such as utilization of biogas, availability resources and investment cost.[39] The biogas upgrading will allow to fulfill the requirements of gas appliances (boilers, engines, vehicles, etc) and increase the heating value of the biogas, which leads to a consistent gas quality, similar to natural gas.[30]

Several biogas upgrading technologies include absorption, Pressure Swing Adsorption (PSA) and membrane separation.[38] In any of these technologies it is crucial to keep low methane losses, mainly because CH_4 is a greenhouse gas 21 times stronger than CO_2.[30]

1.3.1.1. Absorption

Absorption process is based on the solubility of different gases in a liquid scrubbing solution.[37] Usually this process is processed in a column filled with plastic packing allowing to increase the contact between the biogas and the liquid phase.[38] In the column, biogas meets a counter flow of liquid and, since carbon dioxide is more soluble than methane, the liquid will leaving the column with high concentrations of CO_2, while the gas leaving the column will have an increase of methane concentration. This process presents some advantages such as low methane losses (0.1-1.2 %), high methane recovery (> 99%) and allows solvent recovery through a desorption column.[37]

There are different absorption technologies and each one use different absorbents: physical, chemical scrubbing and also water scrubing are some exemples of these technologies.[38]

High pressure water scrubbing (HPWS)

This upgrading technology is the most common used to remove CO_2 from biogas. Water scrubbing employs water as a solvent for dissolving CO_2 at elevated pressures, since solubility of this gas in water is higher than CH_4 (0.035 kg CH_4 per kg water at 17 ºC), particularly at lower temperatures

as can be seen in **Table 1.2**.[38,40] The effluent water that leaves the scrubber column is saturated with CO_2 and can be regenerated using an desorption column and then pumped back to the absorption column. HPWS is an highly efficient process with high methane recovery (> 97%). The main drawbacks of this method are high energy consumption during water regeneration which leads to high operational costs.[39]

Table 1. 2. Solubility, in kg of CO_2 per kg of water at different temperatures (Adapted from Dewil et al. (2008) [30])

	Temperature			
Pressure	**0ºC**	**10ºC**	**20ºC**	**30ºC**
1	0.40	0.25	0.15	0.10
20	3.15	2.15	1.30	0.90
50	7.70	6.95	6.00	4.80

Organic physical scrubbing (OPS)

The process of physical scrubbing is similar to water scrubbing, with the difference that the absorvent is an organic solvent, such as polyethylene glycol (PEG), methanol (CH_3OH) and N-methyl pyrrolidone (NMP), to absorb CO_2.[38,39] Comparing to HPWS, this process is more efficient since CO_2 shows higher solubilities in these organic solvents than in water. The solvents used can also be regenerated by heating or pressure reduce. Selexol® and Genosorb® are examples of commercially available PEG used in organic physical scrubbing.[41] Although it has several advantages such as high methane recovery efficiency (> 97%) and elimination of organic compounds (such as H_2S), the OPS operation process when compared to HPWS, requires more energy for the solvent regeneration and high operational costs since the costs of the organic solvents are significantly higher than water.[39]

Chemical scrubbing process (CSP)

Chemical absorption use amine-based solvents which have high affinity with certain components of a gas mixture.[42] Carbon dioxide, in order to be absorbed in the liquid reacts chemically with the amine in the liquid.[38] This reaction between the gas and the solvent is reversible, being possible solvent regeneration in a desorption column by heating the liquid using steam. Some of the most commonly used solvents are primary amines such as monoethanolamine (MEA), which is a widely used type of amine for CO_2 capture, secondary amines such as diethanolamine (DEA) and tertiary amines such as methyldiethanolamine (MDEA).[43] In order to achieve higher absorption capacities, a mixture of MDEA and piperazine (PZ), called as activated MDEA (AMDEA), was developed.[39]

In CSP methane losses are low (< 0.1%) since the chemical reaction is strongly selective.[38] Despite this advantage, the corrosive properties of amines make this process disadvantageous. CSP is

also energy intensive, mainly for amine regeneration and some part of the amines degrades or is emitted into the atmosphere, which can harm the environment since amines are toxic.[44]

1.3.1.2. Pressure Swing adsorption (PSA)

PSA is the most commonly method used in full scale for CO_2 separation from CH_4 and involves two principal steps, adsorption and desorption.[45] This technology uses an adsorbent material, such as zeolites and activated carbon, that selectively adsorb and desorb the undesired gas components by the variation of pressure. This process take place in vertical columns filled by the adsorptive material as a molecular sieve.[46] The separation of CO_2 occurs under high pressure (adsorption) and the gas with high affinity to the adsorbent remain sticked whereas the others pass. Desorption column allow solvent regeneration by pressure reduction. Through this method, CH_4 recovery rate between 85-90 % can be achieved.[47]

However, CO_2 separation through adsorption method is not considered attractive in large scale since high energy is required for the system, mainly for regeneration and the available adsorbents have low adsorption capacity and selectivity.[43] Another fact that can be seen as a disadvantage is the fact that, in PSA, is necessary a primary step of H_2S removal since this gas is considered toxic to the process and its adsorption is normally irreversible.[39]

1.3.1.3. Cryogenic separation

The biogas separation through cryogenic system operates under a very low temperature and high pressure conditions. These upgrading method is based on the principle that various gases liquefy under different temperature and pressure conditions.[38] The CO_2 and CH_4 boiling points are different, -165.5ºC and -78.2ºC at 1 atm, respectively. Therefore, is possible to separate these two gases by liquefying it. The main disadvantages of this process is the quantity of equipments used that leads to high capital and operational costs and high energy consumption.[39]

1.3.1.4. Membrane separation

Over the past 40 years, membrane separation processes have gained recognition and become part of current market, being one of the most used methods for landfill gas upgrading.[38] Gas separation through membranes consists in using membranes as a selective barrier that transports more easily some gases of the feed mixture than the others due to the different chemical and physical properties of the membrane material and the permeating components (**Figure 1.3**).[39]

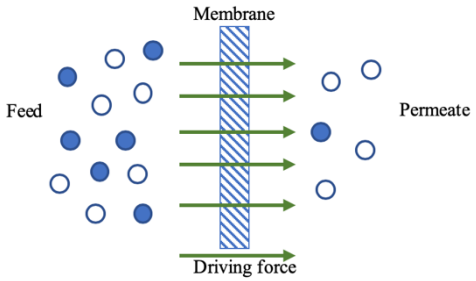

Figure 1. 3. Schematic representation of membrane separation (Adapted from Mulder et al. (2003)[48])

This process works at high pressure (20-40 bar) or at low pressure (8-10 bar) being possible to obtain 92-97% methane content.[37] There are many advantages of membrane separation in biogas upgrading, where the most important include safety and simplicity of the operation, easy maintenance and operation without hazardous chemicals.[49] Furthermore, from the economic point of view, biogas has the perfect composition for the separation to be advantageous through membrane processes, since the volume of gas is relatively low and carbon dioxide content is high.

In order to achieve a viable process, membranes must have a set of characteristics mainly high CO_2 permeability and CO_2/CH_4 selectivity and also chemical and thermal resistance.[50] Several type of membranes can be developed in order to achieve specific features and a separation with a high purity of CO_2.[43] For biogas purification there are three different types of membrane used: polymeric (organic membranes), inorganic or ceramic and mixed matrix membranes (MMMs) which are a combination of polymeric with inorganic fillers.[39,51]

Polymeric membranes

Nowadays, polymeric membranes are the most used for gas separation. These membranes are made from organic materials, such as polyimide (PI), polysulfone (PSf), cellulose acetate (CA) and polymethyl siloxane (PDMS).[39] The use of these membranes for biogas upgrading should always undergo drying prior to membrane separation, since membrane materials are very susceptible to moisture content.[51]

In dense polymeric membranes, the transport of gases through the membrane is based on solution-diffusion mechanism. According to this mechanism, the permeation of molecules through the membrane is controlled by the relation of two major parameters, diffusivity coefficient and solubility coefficient of the different gases.[52] Despite having high mechanical resistance, they possess low thermal and chemical stabilities as well as a trade-off between seletivity and permeability, which means that higher selectivities leads into lower permeabilities and vice-versa.[53,54]

Inorganic membranes

Inorganic membranes are classified as zeolites membranes, ceramic membranes, carbon membranes, metallic membranes or glass membranes, depending on the production material.[53] Normally they present a higher thermal and chemical stabilities than polymeric membranes. Furthermore, they present a higher selectivity, specially for carbon molecular sieves and zeolites. On the other hand, some inorganic membranes have some technical difficulties and problems, such as complicated manufacturing procedures, high manufacturing costs as well as low mechanical properties when compared with polymeric membranes.[52]

Mixed-matrix membranes (MMMs)

Mixed-matrix membranes (MMMs) were developed as an alternative to polymeric and inorganic membranes, combining the advantages and overcome the problems of each. These membranes consist of an inorganic filler (dispersed phase) incorporated into a polymeric matrix (continuous phase).[53] The use of these two materials provides the possibility to the membranes to posses the high mechanical resistance and easy processability of polymeric membranes and the high separation performances of inorganic membranes, which results in a membrane with high separation performace with a potencial to overcome the trade-off for gas separation (**Figure 1.4**).[53,55]

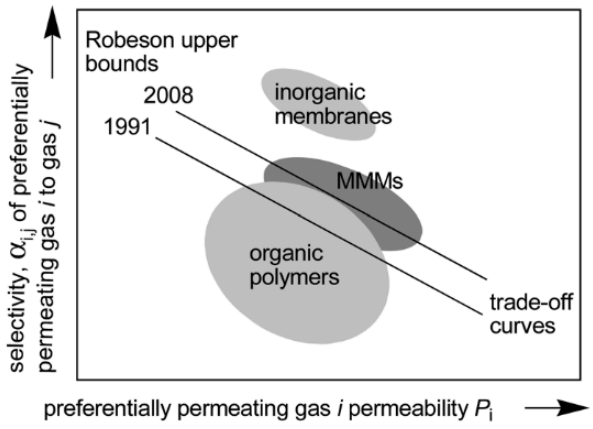

Figure 1. 4. Schematic representation of the relationship between selectivity and permeability with the Robeson upper bound.[53]

The correlation between permeability and selectivity was demonstrated first in 1991 by Robeson with an upper limit, through the analysis of various references about membrane gas separation studies and later updated in 2008. Therefore was possible to discover the relationship between permeability and selectivity that can be graphically represented as upper bound by the log of the separation factor as a function of the log of the higher permeable gas. The Robeson upper bound of 1991 was valid for a variety of gas pairs, including CO_2/CH_4 (**Figure 1.5**).[54] However, the update performed in 2008 allow to introduce another gas pairs.[56] The successful of MMMs preparation depends on the properties of

polymer and inorganic filler used that affect membrane morphology and separations performance. If the affinity between the polymer and the inorganic filler is low, it can result in the formation of voids at the polymer-filler interface.[53] Usually, polymers with highly selective properties lead to better separation performances.

Thus, glassy polymers with a high selectivity are preferred comparing to high permeable rubbery polymers with low selectivity.[57] To choose the inorganic fillers is necessary to considere some properties, mainly their surface and chemical structure as well as particle size distribuition. There are two types of inorganic fillers, porous and non-porous. Porous inorganic fillers are the most used, since they possess high permeability and low selectivity than non-porous. Examples of porous inorganic fillers are zeolites, silica and carbon molecular sieves.[58] As mentioned above, the polymer-filler interactions need to be strong but these materials have shown low compatibilities towards the polymer matrix.

These aspects may be crucial to discover new materials to help answer some of these challenges with high affinity to the polymer matrix, such as metal-organic frameworks (MOFs).[59]

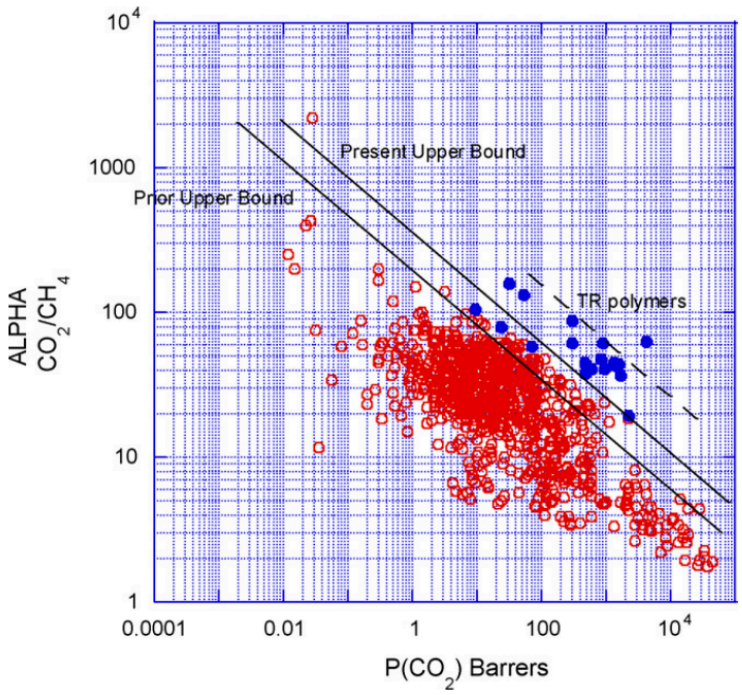

Figure 1. 5. Upper bound correlation between CO_2 and CH_4. [54]

Ionic liquids (ILs)

In the last decade, ILs have gained interest as new functional materials to promote more efficient processes. They can be used in different applications, such as solvents for biological molecules, batteries and fuel cell or carbon dioxide capture processes.

ILs are salts composed of an organic cation and an organic or inorganic anion, which have a melting point lower than 100ºC instead of traditional salts that melts at much higher temperatures.[60] The

low melting point of ILs can be explained by the low intermolecular interactions, low aggregation of their asymmetrical ions and also their charges dislocation.[61,62] These materials have another interesting preperties, such as high thermal and chemical stability, low flammability and low volatility. However, the main characteristic that make them very promising materials is the possibility to enhance their physical and chemical preperties only by changing the cation and anion in their structure. Thus, ionic liquids have been finding an increasing number of applications as "green" solvents. Examples of these applications are organic and chemical chemistry, energy, biotechnology separation processes.[60,62,63] Nowadays, the use of ILs in separation processes is one of the most active areas of reaserch due to the reasons refered above but also because the good levels of solubility and selectivity of CO_2 in these solvents when compared with other gases. For the last one, some studies have been done for the CO_2 solubility in ILs where was concluded that the anion has a dominant role in CO_2 solubility.[63]

Polymeric ionic liquids (PILs) and PIL/IL composite membranes

As referred above, ILs can be applied in a large number of applications. The use of ILs for functional polymers development allowed the appearance of polymeric ionic liquids (PIL)s.

Polymeric ionic liquids, also known as poly(ionic liquid)s or PILs, is a new class of polyelectrolites that results from the introduction of the functional groups associated to ILs into functional polymers. PILs combine the thermal stability and high CO_2 selectivity of ionic liquids (ILs), with the common properties of polymers. Contrary to classic polyelectrolites that are soluble in water, most PILs are only soluble in polar organic solvents.[60] Despite these advantages of using PILs, the low gas permeability and diffusivity through the polymer matrix achieved, led to the development of high performance CO_2 separation membranes and different strategies have been explored using different membrane arragements, such as polymer/IL composite membranes, supported ionic liquid membranes, ion gel membranes and PIL-IL composite membranes.[64]

In PIL/IL composite membranes, the ILs are incorporated into PILs matrix. The development of PIL/IL membranes is an attractive strategy to obtain membranes that combine the best functionalities of both materials, which allow to obtain membranes with enhanced CO_2 transport properties.[65] In order to achieved the maximum CO_2 separation is necessary to take into account the compatibility of both materials. Recently, the incorporation of nanofillers, such as MOFs, has gained interest to improve the CO_2 separation performance of PIL-IL membranes.

Metal-organic frameworks (MOFs)

In the past two decades, MOFs have emerged as a new class of crystalline porous materials and as a potencial fillers in the polymer matrix.[55] Their structure is composed of inorganic metal ions (or metal clusters) connected by means of ligands forming a three-dimentional structure.[66]

MOFs have gained interest as inorganic fillers for MMMs due to their unique characteristics. In addition to their reasonable thermal and mechanical stabilities, the structure of these materials can be adapted to the desired application in terms of pore size and surface area, being possible to enhance their affinity towards different gases.[59,67] In several studies is referred that these materials also reveal capacity for CO_2 removal due to their adsorption selectivities and capacity to CO_2 capture. These properties allow MOFs to have a high potencial where compared to the conventionally used microporous inorganic material such as zeolites.[68] Generally, MOFs has higher porosity and surface area than zeolites, activated carbons and silica gel.[66] Therefore, the challenge in using MOFs in MMMs is to choose the appropriate polymer/MOF combinations for a specific separation.

1.4. Objectives of this thesis

The main objective of this thesis was the development and characterization of new mixed matrix membranes with metal organic frameworks, polymeric ionic liquids and free ionic liquids for the purification of biogas produced from a co-digestion system using an anaerobic co-digestion process.

The first part of this thesis consisted on biogas production through the operation of a single-stage anaerobic system at laboratorial scale treating a mixture of tannery and leachate, increasing the salinity overtime. The increase of salinity can affect negatively the reactor performance, being necessary to control this parameter. Therefore, it is important to study the adaptation of microbial culture to different salinities.

The second part of this work was to prepare and study two groups of new membranes to remove CO_2 from a biogas stream. In the first group, PIL-IL membranes using two different PILs, Poly[pyr_{11}][Tf_2N] and Poly[pyr_{11}][$C(CN)_3$], four ILs, [C_2MIM][Tf_2N], [C_2MIM][$C(CN)_3$], [C_2MIM][BETi] and [C_4MIM][PF_6] and three different solvents, acetone, acetonitrile and DMF, was prepared. In the second group, two MMMs were prepared, namely Poly[pyr_{11}][$C(CN)_3$]/40 [C_2mim][$C(CN)_3$] and Poly[pyr_{11}][Tf_2N]/40 [C_2mim][BETi], with the the metal organic framework (MOF-5).

The membranes prepared were studied to evaluate if the incorporation of MOFs enhanced the membrane properties as well as the CO_2/CH_4 ideal selectivity and CO_2 permeability when compared with the membranes composed only by the PIL-IL.

All membranes were characterized by different methods, namely scanning electron microscopy (SEM) to evaluate their morphology, fourier transform infrared spectroscopy (FTIR) to evaluate ILs and MOF incorporation in PIL, thermogravimetric analysis (TGA) to evaluate their thermal stability, contact angle to determine their hydrophilicity, mechanical properties to evaluate their resistance and flexibility and gas permeation experiments with pure gases (CO_2 and CH_4) at 30ºC.

2. Materials and methods

2.1. Operation of a single-stage anaerobic digestion system

2.1.1. Materials

2.1.1.1. Substrate and inoculum

Leachate and tannery, used as substrates in this study, were provided by Koto, Slovenia. The wastes were previously characterized (see results section) and stored in a refrigerator at 4°C until needed to prepare the influent. The influent was prepared one time per week diluting the tannery with leachate in order to achieve the salinity required (5, 10 or 15 g Na^+ L^{-1}).

The upflow anaerobic sludge bed (UASB) reactor was inoculated with anaerobic granular sludge (30% of working volume) collected from a Biobed Expanded Granular Sludge Blanket (EGSB) reactor treating non saline brewery wastewater (Portugal).

2.1.1.2. Experimental Setup and operation

A single-stage AD system was operated during 61 days in continuous mode at lab-scale with 2.2 L of working volume. The overall system configuration of the UASB reactor is represented in **Figure 2.1**.

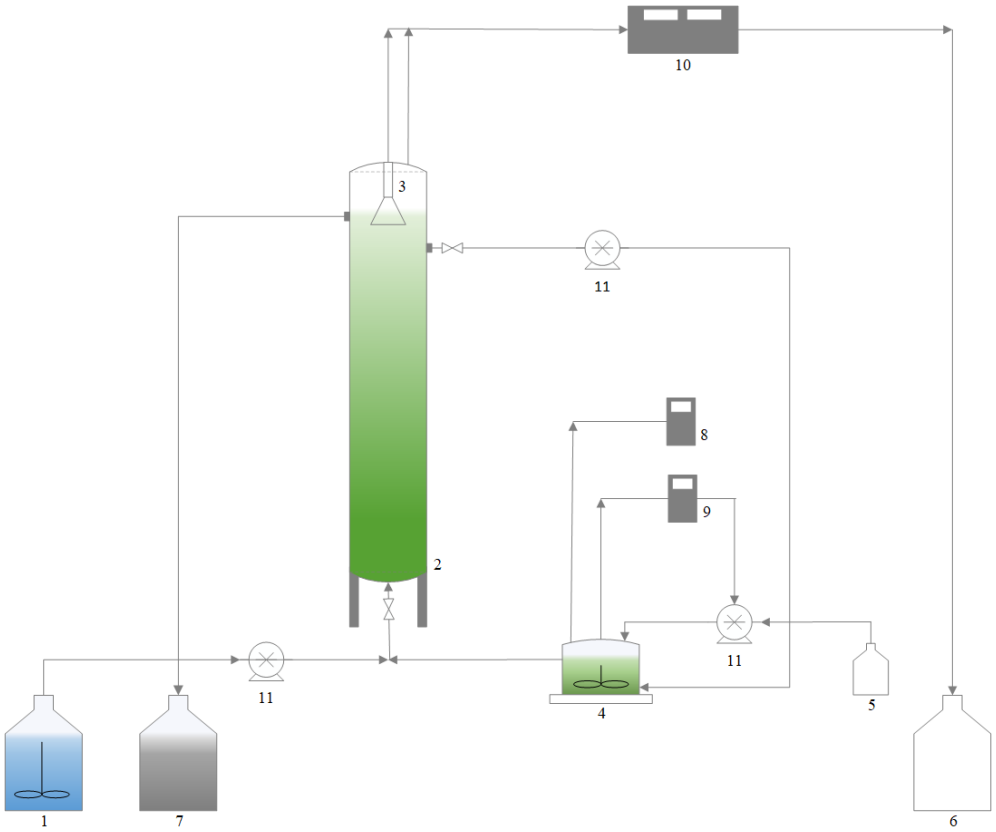

Figure 2. 1. Schematic representation of the single-stage anaerobic system: (1) Influent container; (2) UASB reactor; (3) Gas-liquid-solid separator; (4) pH/redox measure flask ; (5) KOH solution bottle; (6) Biogas container; (7) Clarified fermentation

broth container; (8) Redox controller; (9) pH controller; (10) Gas flow meter; (11) peristaltic pump. Components not shown: water bath system.

The reactor was maintained at 30°C (mesophilic conditions) using a water bath system (CW-05G, Lab. Companion, Jeio Tech, Korea). The pH was automatically controlled 7.07 ± 0.09 by the automatic addition of potassium hydroxide (KOH) 5M. The upflow velocity was maintained at 2 m h^{-1} with a peristaltic pump (Watson-Marlow 323E/D) and the biogas production was measure through a flow meter (*Bioprocess Control*, Sweden).

Table 2. 1. Operational conditions used in the reactor.

Leachate (%)	Tanney (%)	Sodium concentration (g Na^+L^{-1})	Time (d)	pH	HRT (d)	OLR ($gCOD_{soluble}$ $L^{-1}d^{-1}$)
91	9	5	0-5	7	5	2.2 ± 0.3
			6-18	7	3	2.6 ± 1.0
83	17	10	19-42	7	3	3.7 ± 0.1
74	26	15	43-61	7	3	3.7 ± 0.1

The reactor startup conditions were pH of 7.00, redox of -178 mV, HRT of 5 days and OLR of 2.2 ± 0.3 g COD L^{-1} d^{-1}. After the initial acclimatization to the salinity, the HRT was changed to 3 days (maintaining the salinity) in order to increase the amount of wastewater treated and, consequently, the biogas production.

The conditions imposed on the reactor are presented in **Table 2.1**. The reactor was subjected at three different salinities (5, 10 and 15 g Na^+ L^{-1}), obtained through different ratios of leachate:tannery and corresponding to an OLR between 2.2 ± 0.3 and 3.7 ± 0.1 g COD L^{-1} d^{-1}.

2.1.2. Analytical methods

In order to assess reactor stability, standard control parameters were monitored including the quantification of COD, proteins, total suspended solids (TSS) and volatile suspended solids (VSS), nutrients, organic acids (OA) and ions. Sampling (feed and reactor) was performed three times per week and centrifuged at 11.000 rpm during 3 minutes (Micro star 17, VWR, USA). The resulted supernatant was stored at -20ºC until further analysis. To determine TSS and VSS, samples were taken one time per week. In order to control the granular sludge, TSS and VSS samples were taken at various heights (H0, H1 and H2).

Chemical Oxygen Demand

COD is an indirect measurement that allows quantifying the amount of organic matter present in the sample. Through the colorimetric method, COD concentration was measured using *Hach Lange* kits

of the concentration range 0-1000 g L^{-1} O_2. Previously, for soluble COD (SCOD) analysis the samples were pre-treated filtration with a 0.2 µm syringe filter and diluted according to the kit range. Contrarily to soluble COD analysis, the samples for total COD (TCOD) were not filtered. Samples were digested (Hach Lange HT 200S) at 148°C for 120 minutes. Lastly, after cooling at room temperature, COD concentration was measured using a spectrophometer (Hach Lange DR 2800).

Proteins

The protein content was determined according to a modified Lowry Protein Assay method.[69] This colorimetric method is one of the most used to measure the concentration of proteins present in the sample and is based on two main reactions, one is the reaction of protein with copper under alkaline conditions and the other one is the reduction of the phosphomolybdic-phosphotungstic reagent by the copper-treated protein. The reagents used are described in **Table 2.2**. The protein content was determined in feed samples and reactor samples, previously centrifuged, filtered with a 0.2 µm syringe filter and diluted with milli-Q water. Briefly, 1.5 mL of solution C was added to 500 µL of the diluted samples, mixed in the vortex and incubated in the dark for 10 minutes at room temperature. After that, 150 µL of solution D was added, mixed in the vortex and incubated in the dark for 30 minutes at room temperature. Absorbance was measured at λ=750 nm (Hach Lange DR 2800 spectrophotometer) and total protein concentration was calculated through a standard calibration curve of bovine serum albumin (BSA 98%, pH 7.0, Sigma Aldrich) (0 - 100 mg L^{-1}).

Table 2. 2. Reagents used in protein protocol.

Reagents	Composition
Solution A	10g Na_2CO_3 + 0,1g $C_4H_4KNaO_6.4H_2O$ + 500 mL NaOH 0,1M
Solution B	0,5g $CuSO_4.5H_2O$ + 1drop H_2SO_4 + 100 mL H_2O
Solution C	Solution A + Solution B in a proportion of 50:1
Solution D	Folin 50% (v/v)

Total suspended solids (TSS) and volatile suspended solids (VSS)

Total and volatile suspendend solids concentrations (TSS and VSS) were determined for influents and reactor broth once a week and in duplicate according to standard methods[70]. Firstly, the glass fibre filters (VWR, Glass fibre filters 21 mm) were weighed. After this each well-mixed samples was filtered in a vacuum pump (VARIAN - Filtration System), placed in aluminium dishes and dried up overnight at 105°C (Oven TR 60, Nabertherm, Soquimica). The weight of dried sample corresponded to the concentration of TSS. The dried sample was then reduced to ash throughout ignition in a oven (Nabertherm, Soquimica) for 2 hours at 550 °C. VSS concentration was achieved by the difference between the weight of the sample before and after the step at 550 °C.

Nutrients

The concentration of nutrients (NH_3-N and PO_4-P) were obtained by a colorimetry method implemented in a continuous flow analyser (Skalar San ++, Skalar Analytical, Netherlands) with a standard calibration curve of ammonium chloride (NH_4Cl 99%, Sigma) and ortho-phosphoric acid (H_3PO_4 85%, Panreac) at concentrations ranging from 4 to 20 mg L^{-1}. The samples were previously centrifuged (Micro star 17, VWR, USA) and diluted with milli-Q water.

Organic acids analysis by High performance liquid chromatography (HPLC)

Organic acids (acetic, butyric, isobutyric, propionic, valeric and isovaleric acids) were quantified through high performance liquid chromatography (HPLC) using a Biorad Aminex HPX-87H column (300 x 7.8 mm) and a Biorad pre-column (125-0129 30 x 4.6 mm) coupled to an IR detector. The analysis was conducted at 30 °C with sulphuric acid (H_2SO_4 0.01 N) as eluent at a 0.5 mL min^{-1} flow rate. The concentrations of organic acids were calculated through a standard calibration curve (31 - 1000 mg L^{-1} of each organic acid). Sample preparation included the filtration using a syringe filter (0.2 µm pore size filter).

Gas analysis (GC)

In order to analysis the composition of the biogas produced, in terms of CH_4, CO_2, O_2, N_2 and H_2 content, was used gas chromatography (GC). The GC (Angilent Technologies 7890B) was equipped with a TCD detector and 50 meters of CP-Molsieve 5A and 25 meters PoraBOND Q columns. The mobile phase was argon with 5 mL min^{-1} of flow rate. The temperatures of the injection port and the detector were 120 and 70ºC, respectively. Gas samples were collected in a syringe (100 µL) and injected as soon as possible into the equipment.

Ions

The sodium concentration was analysed by inductively coupled plasma-atomic emission spectrometry (ICP-AES). The ICP-AES Horiba Jobin-Yvon Ultima is equiped with a 1.00 m Czerny-Turner monochromator, a RF generator at 40.68 MHz.

The determination of chlorine concentration was performed by DIONEX (ICS3000). The system was composed by a IR-detector, a pre-column (Ionpac AG9-HC) and a column (Ionpac AS9-HC) at 25 °C. The eluent was $NaCO_3$ (9 mM) with a flow rate of 1 mL min^{-1} using a standard concentration range of 10-100 mg L^{-1}.

2.1.3. Parameters calculation

To assess the reactor performance, some parameters were calculated. The removal of organic matter was calculated using **Equation 1**, that relates the soluble COD in the substrate (feed) and in the reactor:

$$COD_{removal} = \frac{[SCOD]_{feed} - [SCOD]_{reactor}}{[SCOD]_{feed}} \times 100$$ (Equation 1)

To determine the CH_4 produtivity were used the **Equation 2** that takes into account the percentage of CH_4 in the produced biogas, the biogas flow rate and the reactor volume. CH_4 yield calculation (**Equation 4**) depends on the same parameters as productivity but also HRT and the difference between de VFA in the feed and in the reactor (ΔVFA), calculated using **Equation 3**.

$$CH_4\ produtivity = \frac{\frac{\%CH_4}{100} \times Q_{CH_4}}{V_{reactor}}\ , \text{in L}\ CH_4\ L^{-1}\ d^{-1}$$ (**Equation 2**)

$$\Delta VFA = VFA_{feed} - VFA_{reactor}, in\ g\ COD\ L^{-1}$$ (**Equation 3**)

$$CH_4\ yield = \frac{\frac{\%CH_4}{100} \times Q_{gas}}{\Delta VFA \times V_{reactor}} \times HRT, in\ \text{L}\ CH_4\ g_{COD}^{-1}$$ (**Equation 4**)

2.2. Biogas upgrading using MMMs with MOFs

2.2.1. Materials

Mixed matrix membranes (MMMs) were prepared using two different polymeric ionic liquids (PIL)- poly(diallylmethylammonium)bis(trifluoromethylsulfonyl) imide, PIL Tf_2N and PIL $C(CN)_3$, four ionic liquids, namely,1-ethyl-3-methylimidazolium bis(trifluoromethylsulfonyl)imide ($[C_2MIM][Tf_2N]$, 1-ethyl-3-methylimidazolium tricyanomethanide ($[C_2MIM][C(CN)_3]$), 1-ethyl-3-methylimidazolium bis (pentafluoroethylsulfonyl) imide ($[C_2MIM][BETi]$) and 1-butyl-3-methylimidazolium hexafluorophosphate ($[C_4MIM][PF_6]$) and the metal-organic framework (MOF-5). Properties of the ILs used were determined and are shown in **Table 2.3**.

Acetone, acetonitrile and *N,N dimethylformamide* (DMF) were used as solvents.

Table 2. 3. Properties results of the ionic liquids used.

Ionic Liquid	wt % of water	Molecular weight ($g.mol^{-1}$)	Density($g.cm^3$) 30ºC	Viscosity (mPa.s) 30ºC
$[C_2MIM][Tf_2N]$	0.19	391.31	1.517	26.172
$[C_2MIM][C(CN)_3]$	0.50	229.28	1.030	11.468
$[C_2MIM][BETi]$	0.31	491.32	1.590	55.951
$[C_4MIM][PF_6]$	2.20	284.18	1.356	72.725

The PILs used contain the same polycation, pyrrolidinium ($[pyr_{11}]$) and two different counter-anions, $[Tf_2N]$ and $[C(CN)_3]$. These PILs were synthesized by an anion exchange reaction using the commercially available polymers lithium bis(trifluoromethylsulfonyl)imide (99 %) and sodium tricyanomethanide (98 %) following an established procedure[71], obtaining a white solid, PIL Tf_2N and PIL $C(CN)_3$, respectively. The polymers were then whashed with milli-Q water and dried at 60ºC until a constant weight was achieved.

Methane (CH_4) (Praxair, USA) with 99.5% of purity and carbon dioxide (CO_2) (Praxair, USA) with 99.998% of purity were used in gas permeation tests.

MOF-5

MOF-5, also known as IRMOF-1 is the most studied MOF with promising industrialization results. The structure of MOF-5 is composed of Zn_4O as metal clusters connected by 1.4 – benzenedicaboxylate (BDC) as linear linkers.[72] The main characteristics of MOF-5 are high thermostability (up to 400 ºC), high porosity and high adsorption capacity for CO_2. Several zinc-based MOF possess high specific surface area, tunable pore size and large accessible pore volume, which make them ideal adsorbents.[73,74] This MOF also belongs to a class of nanoporous coordination polymers

(IRMOFs) characterized by interchangeable organic likers, allowing manipulation of pore size and surface area through the specific ligand selection.[75]

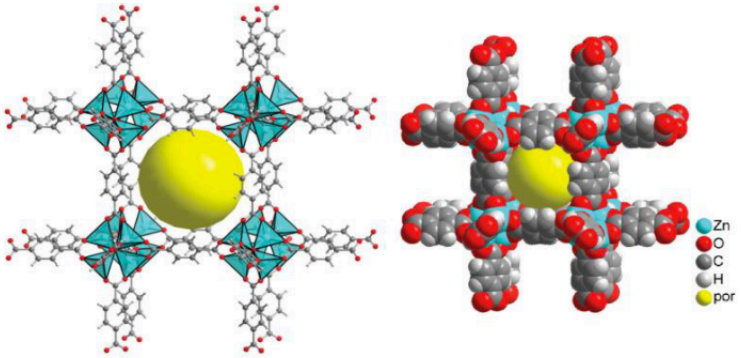

Figure 2. 2. Structure of MOF-5. [76]

2.2.2. Methods

2.2.2.1. MOF-5 synthesis and characterization

For the synthesis of MOF-5, 2.2 g of zinc nitrate hexahydrate, $Zn(NO_3)_2.6H_2O$ (*Sigma-Aldrich,USA, purity* 99.99%), was mixed with 0.92 g of terephthalic acid, H_2BDC (*Sigma-Aldrich, USA*, purity 98%) in 100 mL of N,N-Dimethylformamide, DMF (*Carlo Erba*, France, purity 99.8%) and 2.7 ml of distilled water. The solution obtained was stirred for a sufficient time until complete dissolution and then transferred to an Teflon autoclave and introduced into a high temperature oven (modelo) for 48 hours at 120°C. After cooling at room temperature, the crystals were washed with DMF and dried for 12 hours at 150°C in the oven obtaining about 0.446 g of MOF-5.

In **Table 2.4** are identified the characteristics and the structure of MOF-5.

Table 2. 4. Chemical and physical properties of MOF-5

MOF	Molecular formula	BET Surface area (m^2/g)	Pore size (nm)	Particle size (μm)
MOF-5	$Zn_4O(C_8H_4O_4)_3$	3000 [77]	0.8 [77]	1-2 [78]

Powder X-Ray Diffraction

Powder X-Ray diffraction or PXRD is a commom technique that allows the measurement of diffraction pattern of crystalline materials being possible to verify its composition, purity and structure.

In the scope of this thesis, PXRD data were collected to confirm the crystalline structure of MOF-5. Said spectrum was obtained using a MiniFlex II bentchtop diffractometer (*Rigaku Corporation, Japan*) with CuKα radiation operating at 30 kV and 15 mA and the measuremens for the MOF-5 were carried out between 2º and 70º (2θ) with a step of 0.02º according to Ming et al. 2014.[79]

2.2.2.2. Preparation of PIL-IL composite membranes

PIL-IL composite membranes were prepared through the solvent evaporation method. In **Table 2.5** are present the combination of PIL-IL and the corresponding solvent used in this study.

As a first step, 0.6 g of PIL and 0.4 g of IL were weighed on a balance (BL 120S model) using a vial containing a magnetic stirrer and dissolved in the corresponding solvent (6 % (w/v)). The solution was magnetically stirrer during a few minutes to guarantee the dissolution of the PIL and IL in each solvent. Membranes with PIL $C(CN)_3$ required to be heated during about 15 minutes.

Table 2. 5. Solvents, PIL and IL used to composite membrane preparation

Solvent	Poly(ionic liquid)-PIL	Ionic Liquid-IL
Acetone	PIL Tf_2N	$[C_2MIM][Tf_2N]$
		$[C_2MIM][C(CN)_3]$
		$[C_2MIM][BETi]$
		$[C_4MIM][PF_6]$
Acetonitrile	$PILTf_2N$	$[C_2MIM][Tf_2N]$
		$[C_2MIM][C(CN)_3]$
		$[C_2MIM][BETi]$
		$[C_4MIM][PF_6]$
	PIL $C(CN)_3$	$[C_2MIM][Tf_2N]$
		$[C_2MIM][C(CN)_3]$
		$[C_2MIM][BETi]$
		$[C_4MIM][PF_6]$
DMF	PIL $C(CN)_3$	$[C_2MIM][C(CN)_3]$

The PIL/IL membrane solutions prepared with acetone and acetonitrile were casted in plates over 48 hours. The membrane prepared with DMF were casted in Teflon plates and heated over a period of 8 hours at a constant temperature of 50ºC.

2.2.2.3. Preparation of PIL/IL/MOF-5 mixed matrix membranes

PIL-IL mixed matrix membranes with different MOF-5 concentrations (10, 20 and wt.30%) were also prepared through solvent evaporation method.

Inicially, PIL-IL membrane was prepared as refered above but using only half volume of solvent. Simultaneosly, the addictive solutions were prepared in separate vials dissolving 0.1 g (10 wt.%), 0.2 g (20 wt.%) and 0.3 g (30 wt.%) of MOF-5 in the remaining solvent. All the prepared MOF solutions were sonicated in an ultrasound bath for 4 hours and stirred another 4 hours. Afterwards, the PIL/IL and MOF solutions were mixed and left stirring overnight. Membrane solutions were casted in plates over a period of 48 hours. The membrane solutions using DMF as solvent were casted in Teflon plates and heated over a period of 8 hours at a constant temperature of 50ºC.

2.2.2.4. Scanning Electron microscopy (SEM)

Scanning electron microscopy was performed to evaluate the membranes morphology and the MOF-5 distribution in the polymer matrix. This analysis allows to evaluate if the membrane prepared are porous or dense through their cross-section and surface.

The samples were broken with liquid nitrogen (1x1cm) and treated with a layer of Au-Pd since membranes are not conductive. The analysis was done with a Scanning Electron Microscopy (HITACHI S-2400, 25kV) of Instituto Superior Técnico with the supervision of Dr. Isabel Nogueira.

2.2.2.5. Fourier Tranform Infrared Spectroscopy (FTIR) Analysis

The FTIR analysis was performed in order to confirm the incorporation of IL and MOF in the PIL membranes and also to determine the interactions established between the materials in the membrane. The FTIR spectra of the pure PIL, IL, MOF and the prepared MMMs were acquired using a Perkin Elmer Spectrum two spectrometer. All spectra were collected using 10 scans, from 400 to 4000 cm^{-1}.

2.2.2.6. Contact Angle

The hydrophilicity is a relevant characteristic that needs to be determined for membranes. In this study the technique used consists of contact angle measurement between a drop of water or other solvent and the membrane surface. When the drop of water comes in contact with the membrane surface three interfacial tensions are formed, namely, solid-vapour, solid-liquid and liquid-vapour. To evaluate the hydrophilicity of the prepared membranes milli-Q water was used. Thus, the membranes can be classified as hydrophilic or hydrophobic if the contact angle is inferior or superior to 90ºC, respectively.

Rectangular shaped membrane samples were used and each one was measured four times, using a syringe to place the drop of water in the membrane surface. The final values presented were an average of the four measurements.

The software of KSV (CAM2008) and an optic system was used for contact angles measurements. The optic system allows to capture several images of the drop of water on the membrane surface and the software calculates the left and right angles. The software was defined to capture 10 frames in each measurement.

2.2.2.7. Termogravimetric Analysis (TGA)

Termogravimetric analysis is a thermal analysis technique used to evaluate the thermal stability of a variety of materials that take into account the total weight loss as a function of increasing temperature.

PIL-IL membranes and MMMs were tested using a TA Instrument Model TGA Q50 and heated from room temperature to 600 ºC, at heating rate of 10°C min^{-1}. All the experiments were carried out under a constant nitrogen flow of 40 mL min^{-1}. The results were analysed using a Universal Analysis 4.5 A software.

2.2.2.8. Mechanical properties

Mechanical properties allows to analyse the material behavior when is subjected to external forces and also its ability to resist or transmit these efforts without fracturing or deform.

Puncture test measurements were performed in all the prepared membranes in order to determine the force required to puncture them. These tests were performed using a texturometer analyser (TA XT Plus Texture analyser – Stable Micro Systems, UK) in *Instituto Superior de Agronomia (ISA)*, with the supervison of Dr. Vitor Alves.

The experiments were done at room temperature, using samples with dimensions of 3x3 cm and each sample was replicated three times. The texturometer has a probe with 2mm diameter, which moves at constant speed (1 mm s^{-1}) and perforates the sample. The apparatus is connected with a software that is used to calibrate the equipment and also to record the results.

At the beginning of the test, the probe enters in contact with the sample and the applied force (F) is registed in the software as a function of time (s) and distance (mm). The tensile strength (σ) was calculated through the results of applied force and the probe cross sectional area (S_c). The probe area and tensile strength were calculated using **Equation 5** and **Equation 6**, respectively.

$$S_c = \pi * r^2 \qquad \textbf{(Equation 5)}$$

Where,

S_c – Cross sectional área (m^2)

r – Probe radius (m)

$$\sigma = \frac{F}{S_c} \qquad \textbf{(Equation 6)}$$

Where,

σ - Tensile strength (Pa)

F – Force (N)

S_c - Cross sectional área (m^2)

The elongation was also determined using **Equation 7**.

$$\varepsilon = \frac{l_{final} - l_{initial}}{l_{initial}} \qquad \textbf{(Equation 7)}$$

Where,

ε - elongation

$l_{initial}$ – initial distance (m)

l_{final} – final distance (m)

2.2.2.9. Gas permeation experiments

The main objective of this work was the development of MMMs for CO_2 separation present in biogas streams. Gas permeation experiments allows to simulate the gas stream and determine permeability and selectivity for different gases. In order to measure CO_2 and CH_4 permeabilities a permeation apparatus shown in **Figure 2.3** was used.

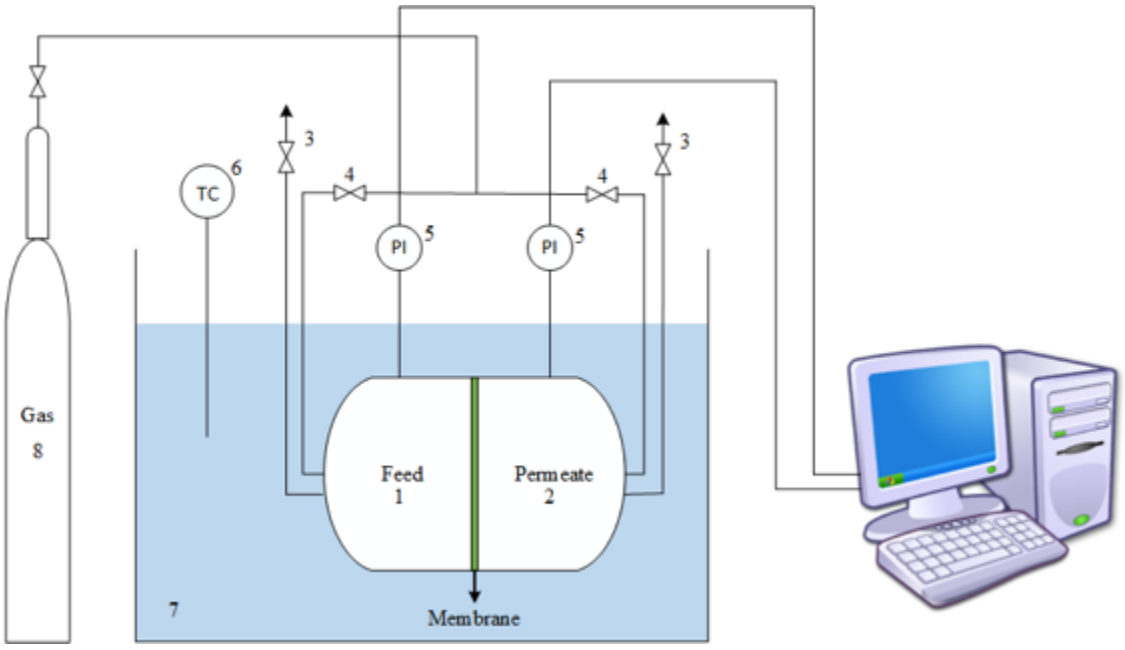

Figure 2. 3. Schematic representation of the single gas permeation installation: (1) Feed; (2) Permeate; (3) Outlet valves; (4) Inlet valves; (5) Pressure indicators; (6) Temperature controllers; (7) Water bath; (8) Test gas. (Adapted from Nesves et al. (2010)[80])

This apparatus is composed by a cell divided in two compartments with the same volume (feed and permeate), a water bath with a thermostat (Julabo ED, Germany) that maintain the temperature at 30°C, two pressure transducers (Druck, PDCR 910 models 99166 and 991675, England) that allows to acquire the pressure of each compartment at every second. *LabView Sofware* was used to monitor the pressure variation.

Initially, the membrane is placed in the cell between the two compartments, dipped in the bath and with all valves open a purge is made in order to guarantee that only the studied gas (CO_2 or CH_4) exist within the cell. The exhaust valves are closed and the cell is fed with a pressure of about 0.7 bar. When the desired pressure is reached, the inlet valves are closed and the pressure is left stabilizing during a few minutes. After, the driving force is made in which the permeate exhaust valve is opened and closed creating a pressure difference between both cell compartments.

Over time it will be observed a gradual decrease in feed pressure values and a increase in permeate pressure values, until the equilibrium is reached.

For the permeability calculations, the time t_0 is considered the time when the driving force is applied. The pressure variation with time in both compartments allowed to obtained gas permeability values, using **Equation 8**. [80]

$$\frac{1}{\beta} * ln\frac{p_{feed_0} - p_{perm_0}}{p_{feed} - p_{perm}} = \frac{1}{\beta} * ln\frac{\Delta p_0}{\Delta \mathrm{p}} = P * \frac{t}{\ell} \qquad \textbf{(Equation 8)}$$

Where,

$\beta - Experimental\ cell\ geometric\ parameter\ (m^{-1})$

p_{feed} – Pressure in the feed compartment (bar)

p_{perm} – Pressure in the feed compartment (bar)

$\Delta p_0 - Pressure\ difference\ at\ t_0 (bar)$

$\Delta \mathrm{p} - Pressure\ difference\ through\ time\ (bar)$

$\mathrm{P} - Permeability\ (m^2 s^{-1})$

$\mathrm{t} - Time\ (s)$

$\ell -$ Membrane thickness (m)

The membrane gas permeability is obtained from the slope of the graph representation of $\frac{1}{\beta} * ln\frac{\Delta P_0}{\Delta P}$ as a function of $\frac{t}{\ell}$.

The geometric parameter β is given by **Equation 9** and depends on the cell used.

$$\beta = A * \left(\frac{1}{V_{feed}} + \frac{1}{V_{permeate}}\right) \qquad \textbf{(Equation 9)}$$

Where,

β - Geometric parameter (m^{-1})

A – Membrane area (m^2)

V_{feed} – Feed compartment volume (m^3)

$V_{permeate}$ – Permeate compartment volume (m^3)

The geometric parameter was determined experimentally using a PDMS membrane with a thickness of 121μm and N_2 permeability already known of $2.3x10^{-10}$ $m^2.s^{-1}$. This calibration was made according to the same protocol used previously for membranes permeation experiments.

With the pressure values obtained through time was possible to determine β that corresponds to the slope of $\frac{1}{P} * ln\frac{\Delta P_0}{\Delta P}$ as a function of $\frac{t}{\ell}$ graph.

The ideal selectivity between gases ($\alpha_{A/B}$) was also determined taking into account the permeability of the two pure gases, A and B, according to the **Equation 10**.

$$\alpha_{A/B} = \frac{P_A}{P_B} \qquad \textbf{(Equation 10)}$$

Where,

$\alpha_{A/B}$ – Ideal selectivity between A and B

P_A – Permeability of A ($m^2\ s^{-1}$)

P_B – Permeability of B ($m^2\ s^{-1}$)

3. Results and discussion

This section is divided in two parts, the first one is relative to the anaerobic reactor performance, including biogas production, composition and COD removal and the second is relative to the MMMs with MOFs characterization.

3.1. AD operation

3.1.1. Leachate and tannery characterization

A mixture of leachate and tannery wastewater was used as substrate for biogas production. Therefore each wastewater was characterized in order to determine the influent dilution for each salinity applied. The composition of each wastewater is presented in **Table 3.1.**

Table 3. 1. Characterization of the different wastewaters treated in the single-stage AD system.

Parameter	Tannery	Leachate
Na^+ (g L^{-1})	58.5	0.5
Cl^- (g L^{-1})	42.6	45.9
PO_4^{3-}-P (mg P L^{-1})	106.5	107.9
NH_4^+-N (mg N L^{-1})	514.8	153.8
Protein (g L^{-1})	2.9	0.8
OA (g L^{-1})	6.9	7.3
Total COD (g COD L^{-1})	9.8	8.1

Through the results was possible to observe the differences between the wastewaters. Besides the organic matter content, in terms of COD, was similar for the two substrates, the amount of sodium (salinity) present in the tannery was more than 100 times higher than the leachate waste. The amount of ammonia (NH_3) was also higher for tannery than leachate as well as organic acids (OA) content. The treatment of tannery waste presents some challenging due to the presence of inhibitory compounds, mainly sodium, in high amounts. On the other hand, the composition of leachate with high organic content and low sodium concentration presents the typical waste characteristics for their degradation and consequently the production of biogas. Therefore leachate and tannery have complementary characteristics allowing to use a co-digestion process, solving the problem of high salinity of tannery wastewater. The comparison of using a simple digester and a co-digester was performed in previous studies and was observed that the use of co-digestion increased biogas production of about 380% when compared with a common digestion technique.[46]

3.1.2. Overall process efficiency

Regarding to the reactor performance, this study was mainly focused on two aspects: biogas production and composition and COD removal since these parameters allow to control the AD process performance.

The biogas production, composition and COD removal were monitored during the reactor operation. The conditions of reactor start-up were HRT of 5 days, OLR of 2.2 ± 0.4 g COD $L^{-1}d^{-1}$ and a feed rate of 0.4 L d^{-1} in order to allow the adaptation of microbial culture to the salinity of 5 g $Na^{+}L^{-1}$.

The results related to the reactor performance are summarized in **Table 3.2**. The start-up strategy used to adapt the microbial culture to differentes salinities proved to be successful, since a high COD removal and biogas production were obtained. After 5 days of operation biogas production was detected and a high conversion of organic acids was observed indicating an efficient activity of microbial community. However, at 15 g Na L^{-1}, a decrease in reactor performance and a granules desintegration was observed (**Figure 3.3**).

Table 3. 2. Reactor performance (COD removal and biogas parameters) under different salinities.

Substrates		Salinity (g Na^{+} L^{-1})	HRT (d)	OLR (g COD $L^{-1}d^{-1}$)	COD removal (%)	Biogas production (L d^{-1})	CH_4 yield (LCH_4 g^{-1} COD)	CH_4 productivity (LCH_4 L^{-1} d^{-1})
Leachate	Tannery							
91%	9%	5	5	2.2 ± 0.3	98.8 ± 0.9	n.a.	n.a.	n.a.
			3	2.6 ± 1.0	70.8 ± 8.8	1.6 ± 0.3	0.29 ± 0.03	0.54 ± 0.01
83%	17%	10	3	3.7 ± 0.1	94.5±0.9	3.0 ± 0.3	0.33 ± 0.03	0.91 ± 0.13
74%	26%	15	3	3.7 ± 0.1	92.1 ± 4.2	1.8 ± 0.2	0.21 ± 0.02	0.48 ± 0.24

3.1.2.1. Consumption of organic acids and COD removal

Organic acids (OA) are important in the production of methane and their concentrations effect the efficiency of AD. The influent and reactor composition in each condition tested are represented in **Figure 3.1**. Almost all OA presents in the inffluent were consumed in the reactor. As shown, the OA profiles in influent was similar with the increase of salinity.

Although, the consumption of OA was observed during the operation (89.4 %) and an accumulation occured with the decrease of HRT and the increase of salinity to 15 g Na^{+} L^{-1}. On the 3rd day a pump problem was detected and the reactor stayed in batch in order to avoid a overloading and inhibition of methanogens. Despite this operational problem the HRT was decreased from 5 to 3 days, the OLR increased and more OA were fed and as such, an accumulation of OA, mainly HBut, was observed. With a increase of sodium concentration from 5 to 10 g Na^{+} L^{-1} and similar OLR, the OA

convertion increased from 76.5 to 97.7%. From day 51 (15 g Na^+ L^{-1}) an increase of HAc and HPr was observed, which could be related to the granules disintegration and a less efficient acetogenic activity. On the other hand, it is expected that HPr would be the last acetate precursor converted since its conversion is the least favourable, leading to their accumulation and consequently affect the microbial community activity.[81] In fact, a decrease in OA convertion was observed (**Table 3.2**). Li et al. (2012)[82] studied the effect of HPr in anaerobic digestion and show that when their concentration is higher than 2.3 g COD L^{-1} can affect methanogenic growth and activity. Since the HPr concentration was remained between 0.52 and 1.65 g COD L^{-1} the reactor performance seemed not be related with the HPr accumulation.

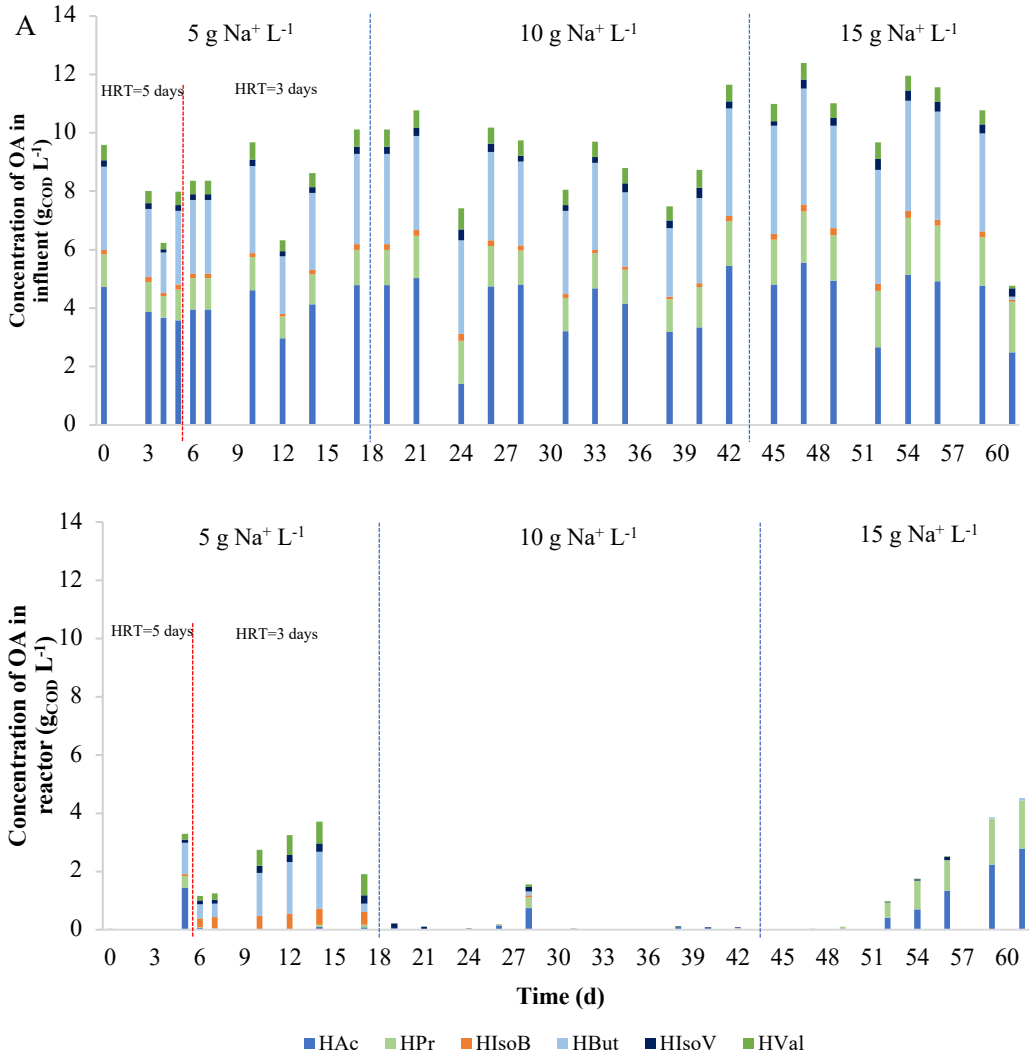

Figure 3. 1. Concentration of OA in influent (A) and reactor (B) obtained for each condition tested.

A similar COD removal were obtained during the reactor operation (**Figure 3.2**). In 12th day, there was a decrease in COD removal, with an accumulation in the reactor due to the adaptation of microbial community to the increase of salt concentration from 5 to 10 g Na^+ L^{-1} . Until 48th day and at

10 g Na^+ L^{-1}, the average COD removal was 94.5 ± 0.9 % (**Table 3.2**). From 54th day a decrese in COD removal and COD accumulation in the reactor was observed, wich can be explained by granules fragmentation, as refered in Section 3.1.2.1. This suggests that the microbial community in the granules was diverse enough to metabolise influents with salinities up to 10 g Na^+ L^{-1}. Parawira et al. (2006)[83] reported a COD removal between 92 ± 4.2 – 98 ± 1.4 % when treating leachate at an OLR between 1.5 - 7.0 g COD L^{-1} d^{-1} and HRT of 13.2 ± 2.9 days which is similar to the results obtained in this study at an OLR between 2.2 ± 0.3 – 3.7 ± 0.1 g COD L^{-1} and HRT between 3-5 days.

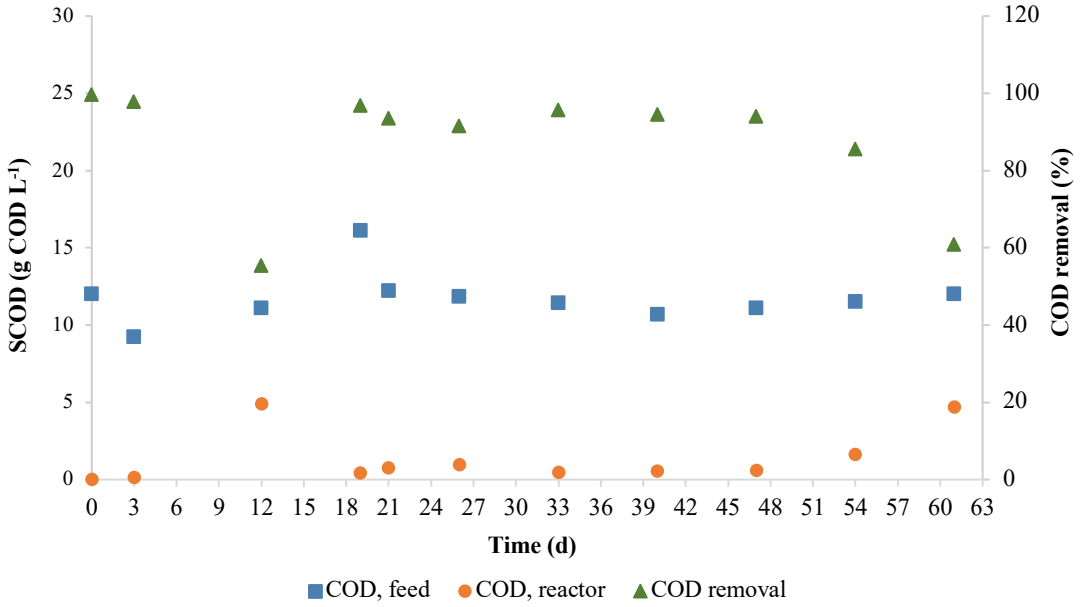

Figure 3. 2. COD variation in the feed and reactor and COD removal during 61 days of operation under different salinities.

3.1.2.2. Granules integrity and biomass concentration

Biogas production and organic matter degradation are directly affected by granules integrity. As reported in some studies, the exposure of anaerobic granules to high salinities can lead to granules disintegration causing wash-out, operational problems and a decrease of reactor performance.[32] Therefore, VSS concentration, at different reactor's heights, was monitored in order to assess the granules integrity and biomass concentration. The average VSS concentration, at different heights, was not constant with the increase of salinity (**Figure 3.3**). At 5 g Na^+ L^{-1} the granules were mainly located at the bottom of the reactor (H0), as expected, which indicates good settling properties. However, at 10 g Na^+ L^{-1} there was a significant decrease in VSS concentration in H0 and a increase in H2, showing that occurred the expansion of the granules. During the operation at 15 g Na^+ L^{-1}, a decrease in granules size comparing to the inoculum was observed, leading to an increase of granules dispersion throughout the reactor. These results demonstrated that the integrity of the granules was affected by salinities above 10 g Na^+ L^{-1}, leading to a granules disintegration and, consequently, the decrease of reactor performance (**Table 3.2**). Lefebvre O. et al (2006)[4] reported that the disintegration of the granules can be explained

as a result of the increase of osmotic pressure that cause death of microrganisms and a reduction in particle size and density.

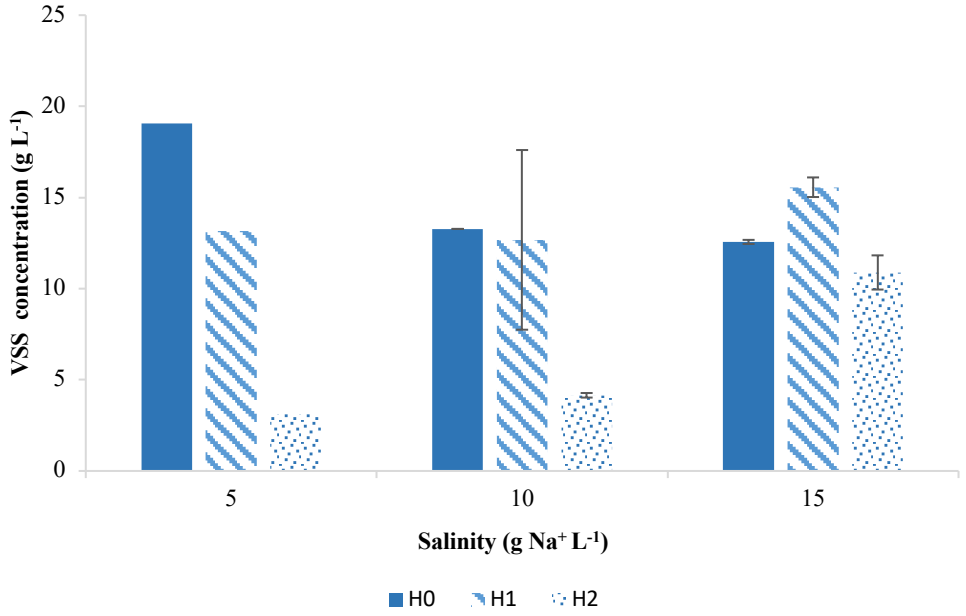

Figure 3. 3. VSS concentration in the reactor at different heights from the bottom of the reactor: H0 (bottom); H1 (middle) and H2 (top). The absence of error bars indicates that the average presented was calculated based on 1 sample.

3.1.2.3. Biogas production and composition

The average biogas production varied between 1.6 ± 0.3 - 3.0 ± 0.3 L d^{-1}, where the highest value was obtained at 10 g L^{-1} (**Table 3.2**).

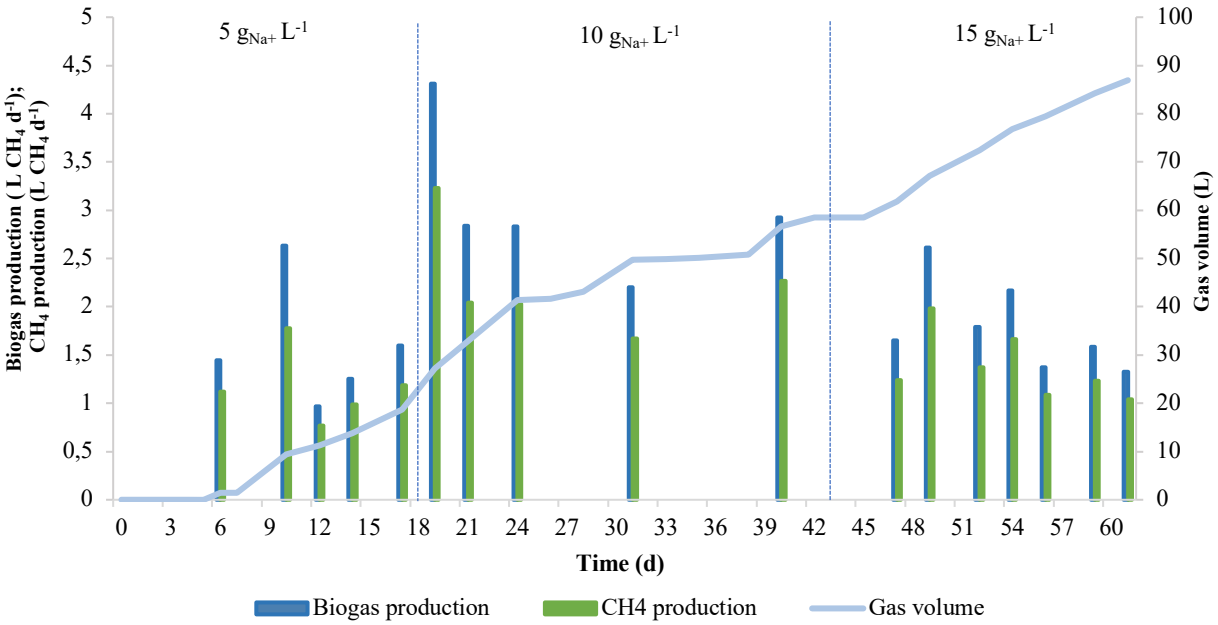

Figure 3. 4. Biogas production, CH_4 production and gas volume over time.

Biogas production increased with the OLR and salinity increase from 5 g Na^+ L^{-1} to 10 g Na^+ L^{-1} (**Figure 3.4**), which is coherent with the high COD removal efficiencies obtained (**Table 3.2**). However, the salinity increase to 15 g Na^+ L^{-1} affected negatively biogas production, which decreased to 1.8 ± 0.2 L d^{-1} (**Figure 3.5**). With the increase of sodium concentration from 5 to 10 g Na^+ L^{-1} and similar OLR, the biogas production increased from 1.6 ± 0.3 to 3.0 ± 0.3 L d^{-1}.

Although salinity affected biogas production, this did not seem to affect their composition. Biogas composition remained fairly stable throught the salinities tested as shown in Figure 3.5. H_2 was never detected in the reactor which suggests that its production rate and its removal rate to produce CH_4 showed unperturbed syntrophic relationships. The average CH_4 content varied between 76.0 ± 3.1% (5 g L^{-1}) and 76.7 ± 1.6% (10 g L^{-1}). These CH_4 content results are higher than other results reported in the literature, which is usually 60% of the biogas. Gebauer (2003)[84] reported a CH_4 content of 50% when treating saline fish farm effluents at an OLR of 1.5 g COD L^{-1} d^{-1} and HRT around 40 days, which is lower to the results obtained in this study.

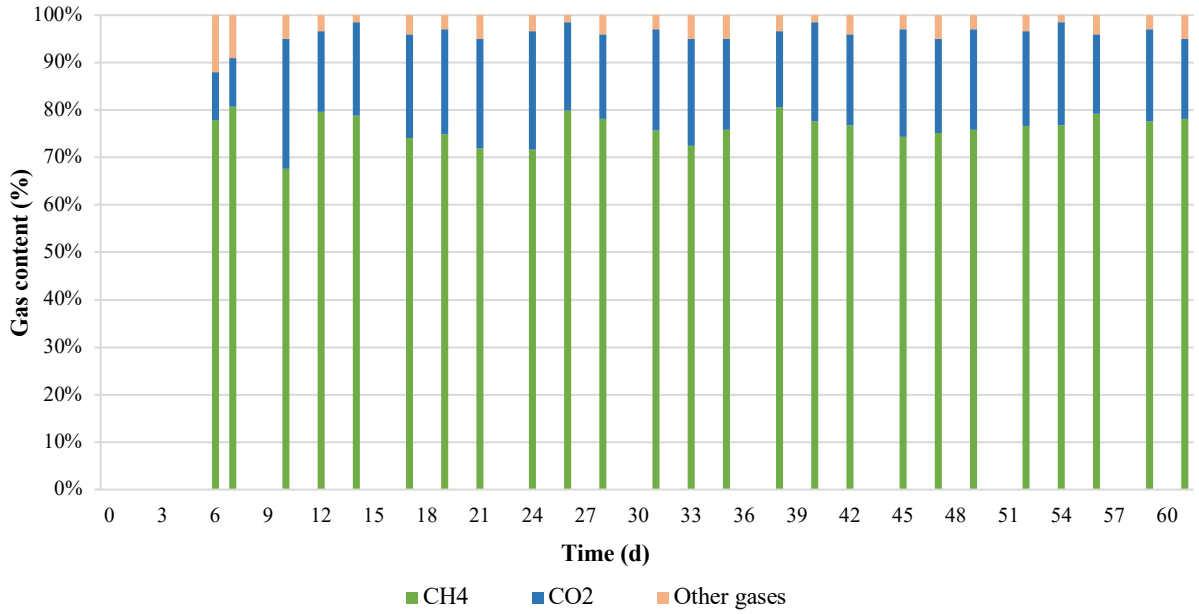

Figure 3. 5. Biogas composition produced in the UASB reactor in each salinity tested. Other gases is refered to H_2 and N_2.

The CH_4 yields obtained in this study were similar to the theroretical value (0.35 L CH_4 g^{-1} COD)[15] and did not vary greatly between conditions (0.21 ± 0.02 - 0.33 ± 0.03 L CH_4 g^{-1} COD) as shown in **Table 3.2**. The decrease of CH_4 yield at 15 g Na^+ L^{-1} prove that there was no evident association between salinity changes and CH_4 yield.

The CH_4 productivity is also perturbed by the increase in salinity, varied between 0.54 ± 0.01 and 0.91 ± 0.13 L CH_4 L^{-1} d^{-1}. The CH_4 produtivity reported by Bouallagui et al. (2004)[85], when treating fruit and vegetables wastes, was 0.52 L CH_4 L^{-1} d^{-1} at an HRT of 8.6 days and OLR of 1.65 g COD L^{-1} d^{-1}, which is similar with the results obtained in this study. It is important to make sure that, despite of

effluents compared are not the same, can be concluded that the increase of salinity do not effect the CH_4 productivity.

3.1.2.4. Nutrients concentration

Phosphorus (PO_4-P) and ammonia (NH_3-N) were measured to assess the microbial growth and nutrient limitation (**Figure 3.6**). There was no indication of nutrient limitation throughout the operation showing that the nutrients present in the influent were enough for the microbial community. PO_4-P concentration in influent remained constantly higher than its concentration in the reactor throughout the operation as shown in Figure 3.6. However, the concentration of ammonia was higher in the reactor than in the influent. In fact, the degradation of proteins causes the release of ammonia which can explained the higher content of ammonia in the reactor. The presence of high amounts of ammonia can causes the inhibitions of AD, mainly methanogenesis, as referred by Lefebvre et al. and references therein.[4]

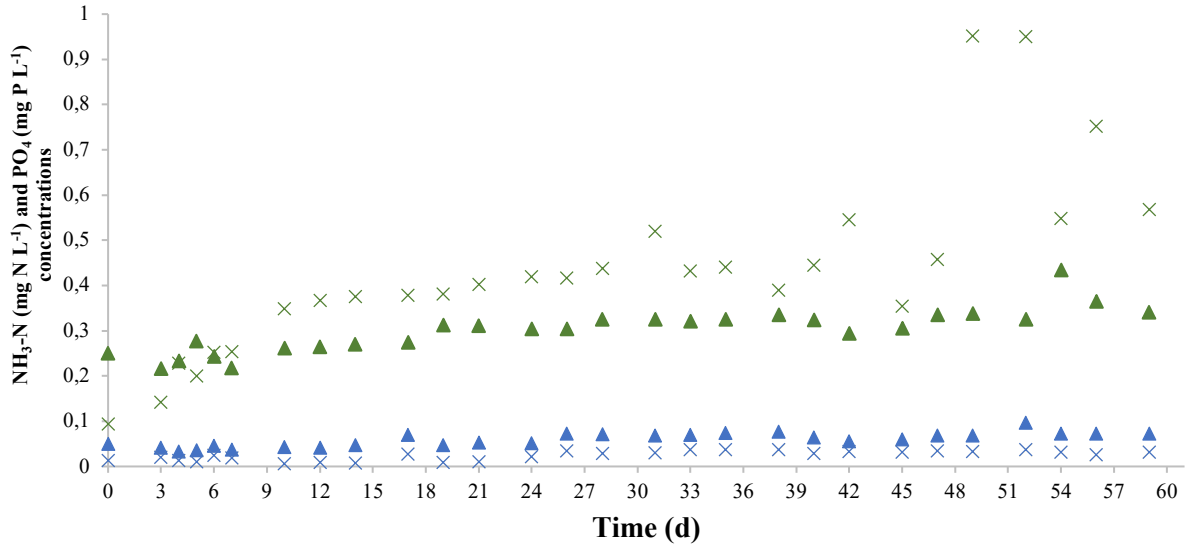

Figure 3. 6. Phosphorus (blue) and amomonia (green) concentrations in the influent (▲) and in the reactor (×) during the 61 days of operation under different salinities: 5, 10 and 15 g L^{-1}.

On the other hand, according to the Xiao Y. et al (2010) study, this inhibition just occurs if the concentration of NH_3 is higher than 100 mg NH_3 L^{-1}.[86] For that reason, we can conclude that the ammonia concentration in the reactor was not inhibitory for methanogenic organisms.

3.2. Biogas upgrading – Performance assessment of MMM's with MOF-5 on CO_2/CH_4 separation

3.2.1. MOF-5 characterization

In this thesis, the MOF-5 was characterized by powder x-ray diffraction (PXRD), fourier transform infrared Spectroscopy (FTIR) and thermogravimetric analysis (TGA).

MOF-5 was used as inorganic filler in a polymeric matrix for MMMs production. These MOF was chosen based on promising results in CO_2/CH_4 separation, with high adsorption properties towards CO_2 when compared to CH_4.[74]

3.2.1.1. Powder X-ray diffraction (PXRD)

As mentioned in section 2.2.1 power x-ray diffraction (PXRD) allowed to confirm the crystalline structure and surface area of MOF-5. As shown in Figure 3.9, PXRD pattern of MOF-5 showed sharpened appearance of peaks, confirming MOF-5 crystallinity.[87] The exposure to water during synthesis and after evacuation can effect MOF-5 morphology, since MOF-5 is water sensitive. The presence of water in porous MOF-5 structure leads to surface area losses. According to previous studies, the presence of water can be confirmed to the appearance of a peak at 8.9º and also by the decrease in peaks intensity at 6.9º and 9.7º.[88] Through the analysis of **Figure 3.7** can be observed that the synthetized MOF-5 present residual water, since the peaks refered above are present.

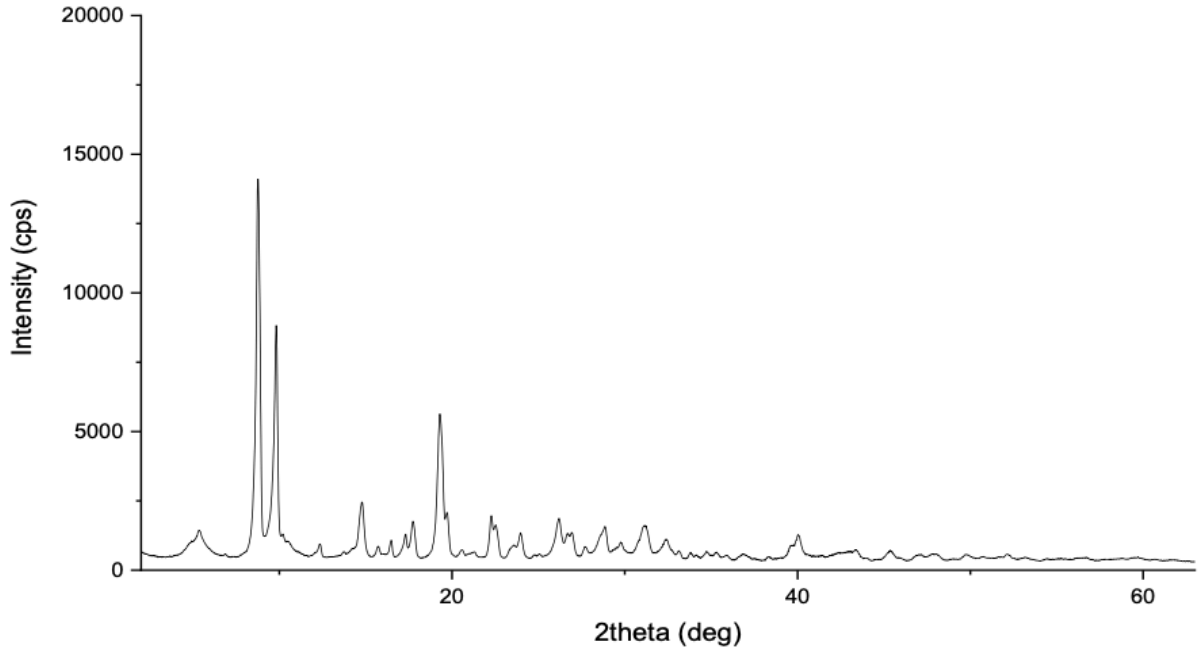

Figure 3. 7. PXRD pattern of the synthesised MOF-5.

3.2.2. Mixed matrix membranes characterization

In **Table 3.3** shows the results of the prepared PIL/IL composite membranes using solvent evaporation method. The combinations of PIL Tf_2N/40 $[C_2MIM][C(CN)_3]$_acetone, PIL Tf_2N/40 $[C_4MIM][PF_6]$_acetone and PIL Tf_2N/40 $[C_2MIM][C(CN)_3]$_acetonitrile were unsuccessful and did not form film.

Table 3. 3. Combinations of solvents, PIL and IL used in the prepared PIL/IL composite membranes and the results of PIL/IL membranes preparation: (✕)did not form film; (✓) formed film.

Solvent	Poly(ionic liquid)-PIL	Ionic Liquid-IL	Results
Acetone	PIL Tf_2N	$[C_2MIM][Tf_2N]$	✓
		$[C_2MIM][C(CN)_3]$	✕
		$[C_2MIM][BETi]$	✓
		$[C_4MIM][PF_6]$	✕
Acetonitrile	PILTf_2N	$[C_2MIM][Tf_2N]$	✓
		$[C_2MIM][C(CN)_3]$	✕
		$[C_2MIM][BETi]$	✓
		$[C_4MIM][PF_6]$	✓
	PIL $C(CN)_3$	$[C_2MIM][Tf_2N]$	✓
		$[C_2MIM][C(CN)_3]$	✓
		$[C_2MIM][BETi]$	✓
		$[C_4MIM][PF_6]$	✓
DMF	PIL $C(CN)_3$	$[C_2MIM][C(CN)_3]$	✓

Therefore, all the successful prepared PIL/IL membranes and MMMs using three MOF-5 loadings (10, 20 and 30 wt%) were characterized by Scanning electron microscopy (SEM), fourier transform infrared spectroscopy (FT-IR), Contact Angle, Thermogravimetric Analysis (TGA) and Mechanical Properties. Gas permeation experiments were also used with CO_2 and CH_4 for all membranes, with the exception of PIL $C(CN)_3$/40 $[C_2MIM][C(CN)_3]$ _DMF, which could not be prepared to the required dimensions. The following results are only refer to PIL Tf_2N/40 $[C_2MIM][BETi]$_acetone and PIL $C(CN)_3$/40 $[C_2MIM][C(CN)_3]$ _DMF, since these PIL/IL membranes were choosen to incorporate MOF-5.

3.2.2.1. Scanning Electron microscopy (SEM)

Usually, membranes used in biogas upgrading are dense. Scanning electron microscopy (SEM) analysis allows the observation of membrane morphology and evaluate the interaction between PIL/IL and MOF-5. The images were obtained for surface and cross-section of the prepared membranes using four different magnifications for each, x500, x1.000, x2.000, x5.000 and x100, x300, x500 and x800,

respectively. The follow imagens present the surface and cross-section with a magnification of x5.000 and x800, respectively.

Table 3. 4. SEM images of PIL Tf_2N/40 [C_2MIM][BETi]/MOF-5 (0, 10, 20 30 wt%) membranes surface and cross-section with a magnification of x5000 and x800, respectively.

wt% of MOF-5	Surface	Cross section
0%	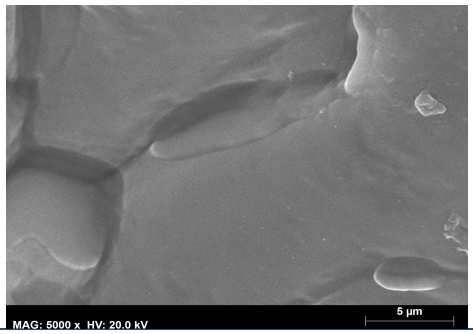	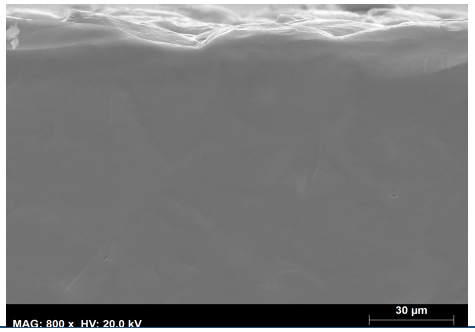
10%	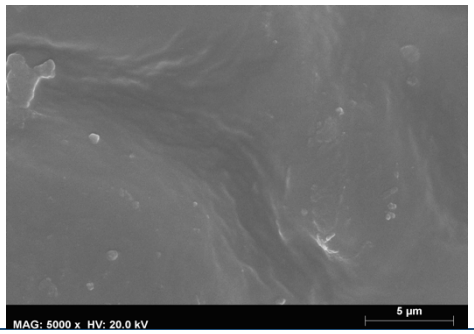	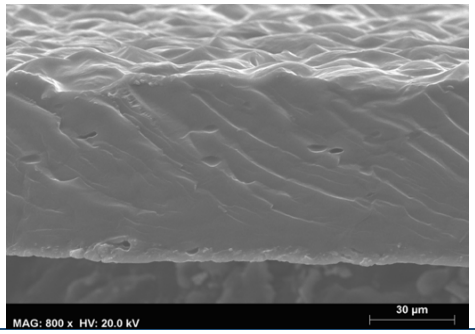
20%	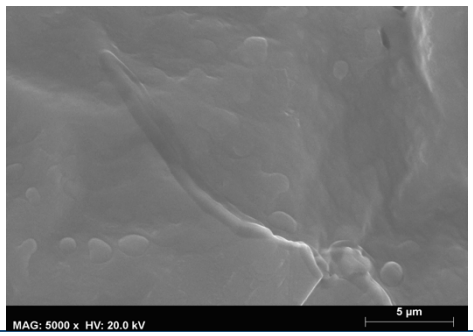	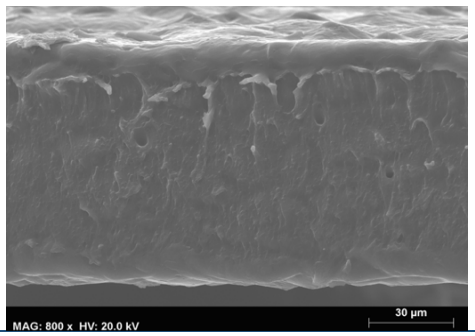
30%	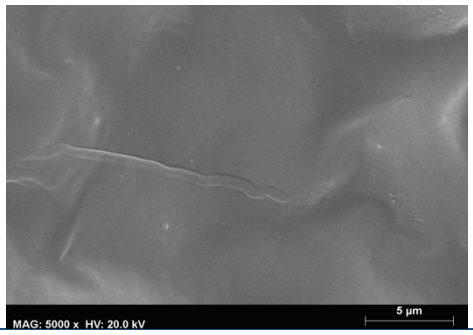	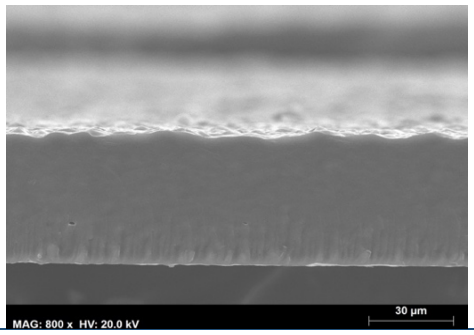

Table 3. 5. SEM images of PIL $C(CN)_3$/40 $[C_2MIM][C(CN)_3]$/MOF-5 (0, 10, 20 30 wt%) membranes surface and cross-section with a magnification of x5000 and x800, respectively.

wt% of MOF-5	Surface	Cross section
0%	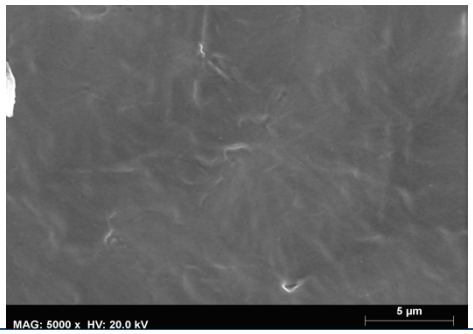	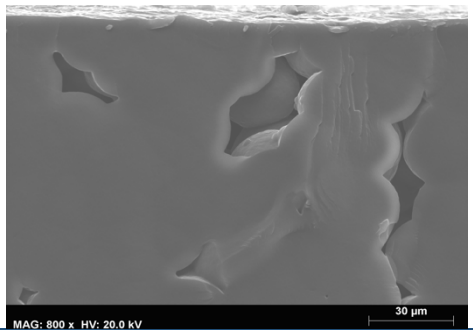
10%	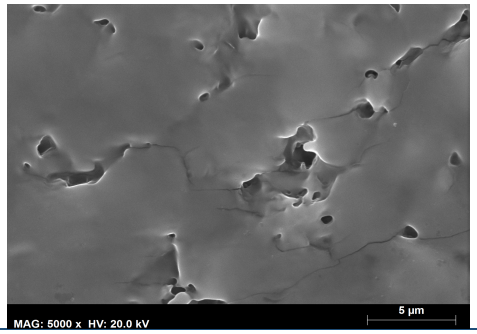	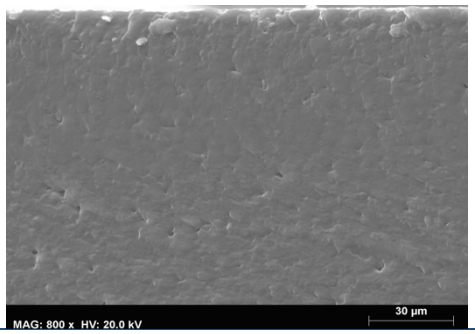
20%	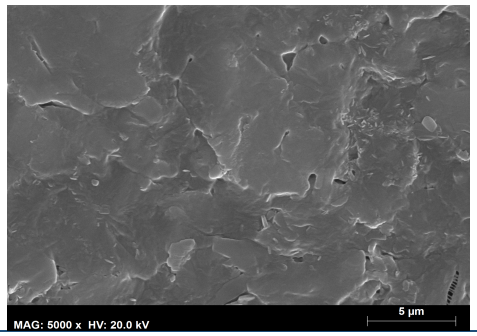	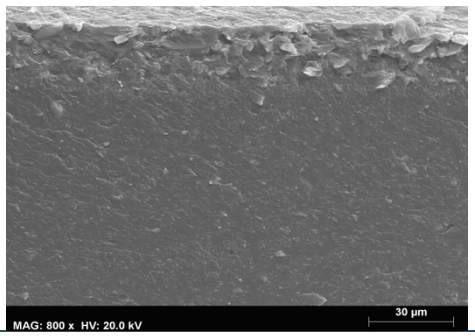
30%	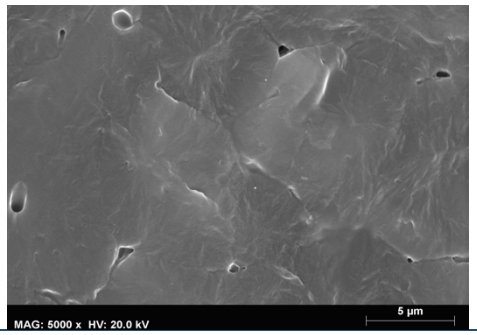	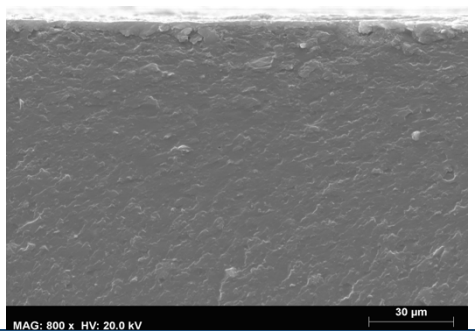

Table 3.4 shows the SEM surface and cross section images of the PIL Tf_2N/40 IL BETi membrane and the respective MMMs comprising 10, 20 and 30 wt% of MOF-5. The PIL/IL membrane surface presents some cavities but these cavities were not observed in the cross-section image. The increase of MOF-5 loading improved the membranes surface morphology, which presented a homogenous surface without the presence of any agglomerates. Furthermore, the prepared MMMs cross-section showed no agglomerates or deformations, obtaining a dense morphology and a uniform dispersion of the MOF into the PIL/IL matrix, being possible to conclude that was possible to successfully incorporate MOF-5 particles into the PIL-IL matrix for all the MOF-5 loading tested. Note that, for MMMs with 10 and 20 wt% of MOF-5 loading, it is possible to identify some randomly distributed voids, which are probably related with the acetone evaporation rate during the membranes preparation.

The SEM images of PIL $C(CN)_3$/40 $[C_2MIM][C(CN)_3]$ and the respectives MMMs are represented in **Table 3.5**. The membrane composed by PIL $C(CN)_3$/40 $[C_2MIM][BETi]$ (represented as 0 wt% MOF-5) presents a homogenous surface without the formation of agglomerates or agglomerates, however, their cross section presents some voids, which can be related with the DMF evaporation rate during the membrane preparation. Regarding PIL/IL/MOF-5 membranes, they posses non-homogenous surface, with the appearance of voids. From the analysis of cross-section images is possible to observe that besides a non-homogenous surface, the membranes exhibit some agglomerates of MOF-5. These fact can be related with a poor interaction between PIL/IL and MOF-5. As reported in previous studies, the different properties of inorganic filler particles and polymer matrices can lead to the formation of non-ideal morphologies such as voids that indicate poor adhesion between inorganic and polymeric phases.[89]

Nevertheless, all the prepared membranes have a dense structure, which is one of the requisites for biogas upgrading process, despite the appearance of some voids.

3.2.2.2. Fourier Transform Infrared Spectroscopy (FTIR) analysis

As mentioned in section 2.2.2.5, FT-IR allows the identification of organic/inorganic species in a certain material. Through the graph of transmittance as a function of the wavenumber was possible to confirm the chemical structure of the prepared PIL/IL/MOF-5 membranes. As a means of comparison, the FT-IR spectra of the MOF-5, IL and PIL/IL used are also illustrated.

The FT-IR spectra of PIL Tf_2N/40 $[C_2MIM][BETi]$/MOF-5 are depicted in **Figure 3.8**. The infra-red patterns obtained for MOF-5 was compared to those previously published in the literature, showing to be similar.[72] The absorption peaks at around 466 cm^{-1} and 522 cm^{-1} are associated to the Zn-O vibrations of the Zn_4O cluster. The vibration bands located between 750 and 1016 cm^{-1} are characteristic of terephthalate compounds. Moreover, the absorption bands at 1390 cm^{-1} and 1503-1586 cm^{-1} are associated to the carboxylic (COO) asymmetric and symmetric stretching, respectively.

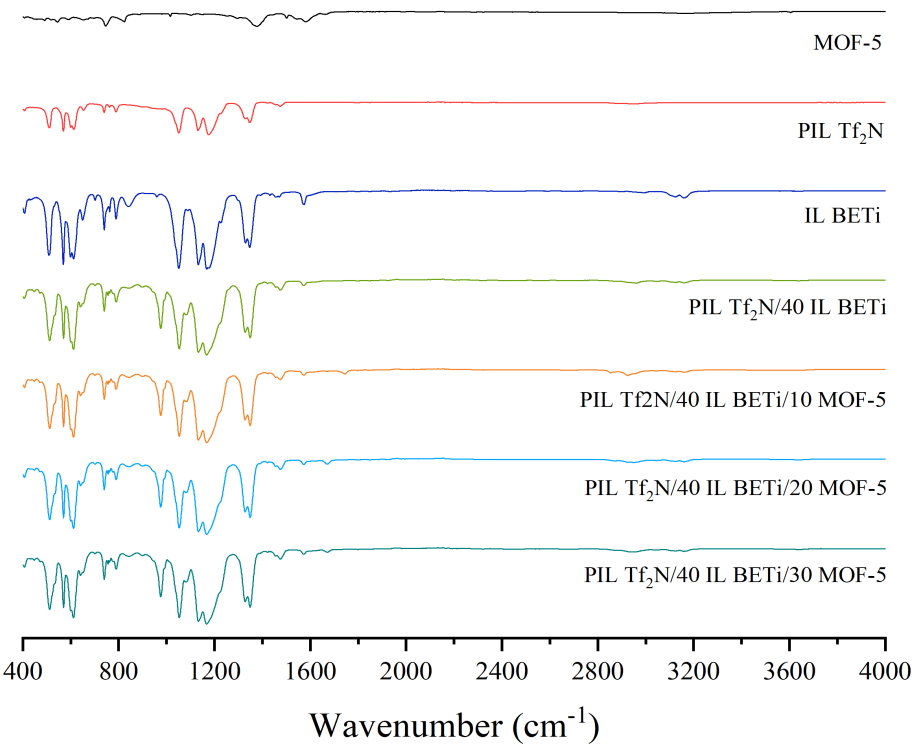

Figure 3. 8. Obtained FT-IR spectra of the studied MOF-5, [C_2MIM][BETi] IL, [pyr_{11}][Tf_2N] PIL, PIL Tf_2N/40 [C_2MIM][BETi] and MMMs with different MOF-5 loadings (10, 20 and 30 wt%).

In PIL Tf_2N/40 [C_2MIM][BETi] spectra the appearance of small bands between 3150 and 2880 cm^{-1} are assigned assigned to CH_2 stretching vibrations, while the peak observed at 1478 cm^{-1} is associated to the CH_3 bending vibrations created from the pendant methyl groups of the pyrrolidinium polycation.[65] According to the literature, the absorption bands at 1347, 1170, 1133 and 1053 cm^{-1} correspond to the $[Tf_2N]^-$ counter-anion of the PIL.[90] The presence of peaks at 1084 cm^{-1} and 975 cm^{-1} are associated to C-N stretching and C=C bending, respectively, which confirms the incorporation of the [C_2MIM][BETi] IL in the PIL/IL membrane.

The FTIR spectra of the PIL $C(CN)_3$/40 [C_2MIM][$C(CN)_3$] and the respectives PIL/IL/MOF-5 mixed matrix membranes are illustrated in **Figure 3.9**. The absorption bands detected at 2154 cm^{-1} are associated to the to C≡N stretching vibrations, which indicates the successful incorporation of the $[C(CN)_3]^-$ cyano functionalized counter-anion.[71] The region between 1600 to 1320 cm^{-1} are originated from the vibrations of the $[C_2MIM]^+$ cation and also the pendant methyl groups of the pyrrolidinium polication. The vibrations observed below 1320 cm^{-1} are derived from the different IL cation and anion and are present in both PIL/IL and PIL/IL/MOF-5 membranes, which confirm the success of the IL incorporation into PIL matrix and as well PIL/IL/MOF-5 mixed matrix membranes.[91]

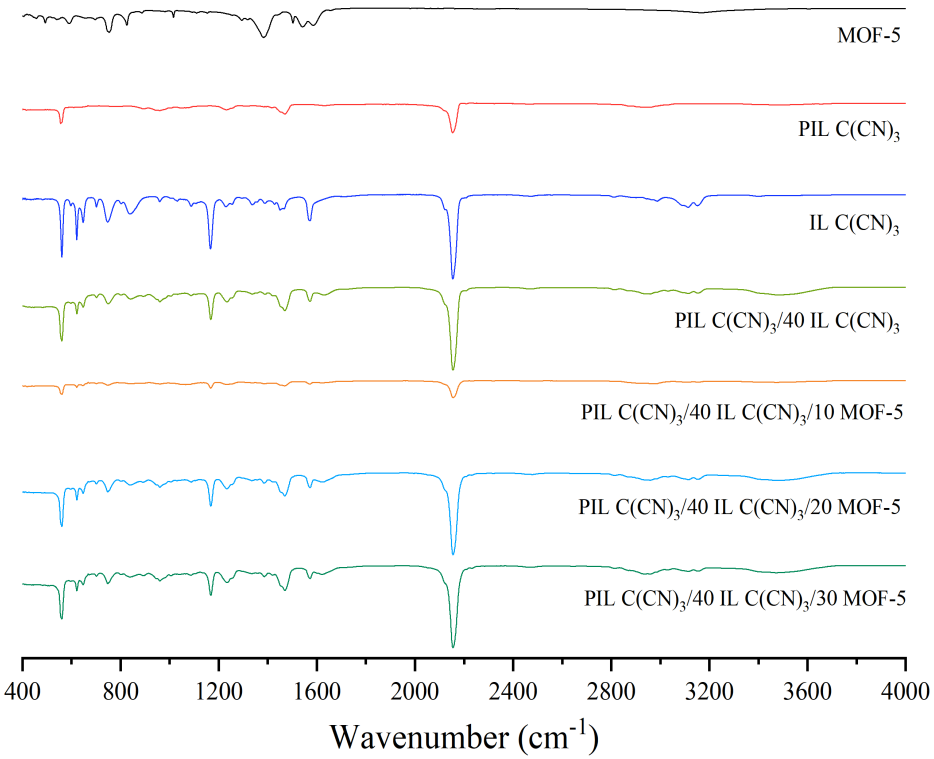

Figure 3. 9. Obtained FT-IR spectra of the studied MOF-5, [C_2MIM][C(CN)$_3$] IL, [pyr$_{11}$][C(CN)$_3$] PIL, PIL C(CN)$_3$/40 [C_2MIM][C(CN)$_3$] and MMMs with different MOF-5 loadings (10, 20 and 30 wt%).

The FT-IR spectra of the MMMs prepared with different amounts of MOF-5 (10, 20 and 30 wt%) did not show significant changes in the absorption bands when compared to the PIL/IL membranes spectrum. This fact could be related with the superposition of the characteristic bands of both PIL/IL membranes and MOF-5.

3.2.2.3. Contact Angle

The contact angles measurements (see section 2.2.2.6) were performed in order to evaluate the membranes hydrophilicity. In this thesis, the measurements were made using water, being the membranes classified as hydrophofic when the contact angle is superior to 90º and hydrophilic if the angle is inferior to 90º. The results of PIL C(CN)$_3$/40 [C_2MIM][C(CN)$_3$] membrane and their MMMs are not presented as they demonstrate high hydrophilicity and contact angle results could not be obtained.

The water contact angles obtained for the PIL Tf_2N/40 [C_2MIM][BETi] and their PIL/IL/MOF-5 are shown in **Table 3.6**. The results revealed a hydrophilic nature of PIL Tf_2N/40 [C_2MIM][BETi] since the contact angle average was 84.5 ± 1.0. The incorporation of MOF-5 into the PIL/IL matrix did not significantly change the contact angle. This result was expected since MOF-5 is hydrophilic due to the easy penetration of water molecules in MOF-5 pores, as refered in previous studies.[75] Thus the hydrophilic character remaind in the prepared PIL/IL/MOF.

Table 3. 6. Water contact angles of the PIL Tf_2N/40 [C_2MIM][BETi] membrane, as well as their MMMs with different MOF-5 loadings (10, 20 and 30 wt%).

Samples	Water contact angle (º)
PIL Tf_2N/40 [C_2MIM][BETi]	84.5 ± 1.0
PIL Tf_2N/40 [C_2MIM][BETi]/10 MOF-5	83.9 ± 0.4
PIL Tf_2N/40 [C_2MIM][BETi]/20 MOF-5	77.6 ± 0.56
PIL Tf_2N/40 [C_2MIM][BETi]/30 MOF-5	82.6 ± 0.4

3.2.2.4. Termogravimetric analysis (TGA)

As mentioned in section 2.2.2.7, thermogravimetric analysis was used in order to evaluate the thermal stability of the prepared MMMs and also, MOF-5 and PIL/IL. Thereby was possible to analyze the effect of MOF-5 concentration increase in membranes thermal stability.

In **Figure 3.10** and **Figure 3.11** the results of PIL Tf_2N/40 [C_2MIM][BETi] and PIL $C(CN)_3$/40 [C_2MIM][$C(CN)_3$] with MOF-5, respectively, are represented. The thermal decomposition values, determined in terms of onset (T_{onset}) and decomposition (T_{dec}) temperatures, are presented in **Table 3.7.**

Table 3. 7. Thermal properties of the PIL Tf_2N/40 [C_2MIM][BETi] membrane, as well as their MMMs with different MOF-5 loadings (10, 20 and 30 wt%).

Samples	T_{onset} (ºC) [a]	T_{dec} (ºC) [b]
MOF-5	245	475
PIL Tf_2N/40 [C_2MIM][BETi]	399	420
PIL Tf_2N/40 [C_2MIM][BETi]/10 MOF-5	373	402
PIL Tf_2N/40 [C_2MIM][BETi]/20 MOF-5	383	412
PIL Tf_2N/40 [C_2MIM][BETi]/30 MOF-5	378	407
PIL $C(CN)_3$/40 [C_2MIM][$C(CN)_3$]	303	511
PIL $C(CN)_3$/40 [C_2MIM][$C(CN)_3$]/10 MOF-5	279	489
PIL $C(CN)_3$/40 [C_2MIM][$C(CN)_3$]/20 MOF-5	279	449
PIL $C(CN)_3$/40 [C_2MIM][$C(CN)_3$]/30 MOF-5	279	573

[a] T_{onset} (onset temperature) defined as the temperature at which the baseline slope changes during the heating.

[b] T_{dec} (decomposition temperature) defined as the temperature at 50% weight loss.

The degradation profile of MOF-5 (**Figure 3.10** and **Figure 3.11**) presents a first weight loss between 150-225 ºC, which probably corresponds to the evaporation of DMF solvent and possibly adsorbed water molecules and the material decomposition occurred in the range of 200-490 ºC. These results are in agreement with those published in the literature.[72]

Through the analysis of **Figure 3.10** is possible to observe that all prepared membranes presented a similar profile up to 200ºC. Besides, were not observed significant weight variations beyond some residual solvent or possible moisture losses. In **Table 3.7** can be seen the effect of MOF-5 incorporation into PIL/IL membrane. The T_{onset} slightly decrease from 399 ºC for the PIL Tf_2N/40 [C_2MIM][BETi] membrane to 373 ºC upon the incorporation of MOF-5. As shown in **Figure 3.9**, above these values all the membranes manifest a pattern of continuous weight loss resulting in complete degradation of the materials. As for T_{onset}, T_{dec} decreased from 420 ºC for the PIL/IL membrane to 402 ºC with the incorporation of 10 wt% of MOF-5.

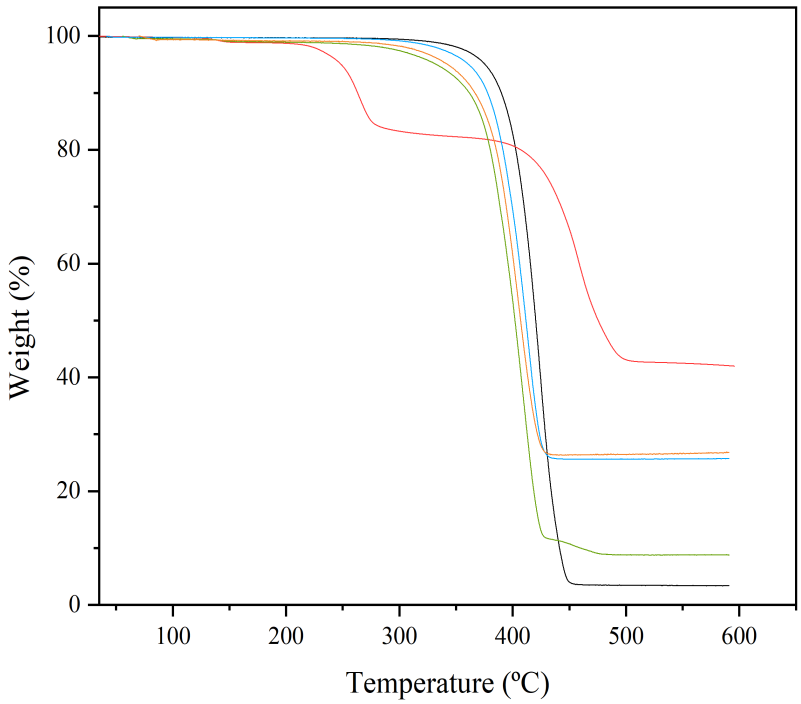

Figure 3. 10. Weight loss as a function of temperature of PIL Tf_2N/40 [C_2MIM][BETi] (black); MOF-5 (red); PIL Tf_2N/40 [C_2MIM][BETi]/10 MOF-5 (green); PIL Tf_2N/40 [C_2MIM][BETi]/20 MOF-5 (blue); PIL Tf_2N/40 [C_2MIM][BETi]/30 MOF-5 (orange).

The profiles of PIL $C(CN)_3$/40 [C_2MIM][$C(CN)_3$] and the respectives PIL/IL/MOF-5 are shown in **Figure 3.11**. The prepared membranes show a similar profile up to 280 ºC, with a slight weight loss due to some residual DMF or possible moisture losses. Looking at **Table 3.7**, it can be seen that the T_{onset} slightly decreased from 303 ºC for the PIL $C(CN)_3$/40 [C_2MIM][$C(CN)_3$] membrane to 279 ºC upon the incorporation of the three MOF-5 loadings. The T_{dec} also decrease with the incorporation of MOF-5, from 511 ºC (PIL/IL) to 489 ºC (PIL/IL/10 MOF-5). However, an increase of T_{dec} was observed after the incorporation of 30 wt% of MOF-5.

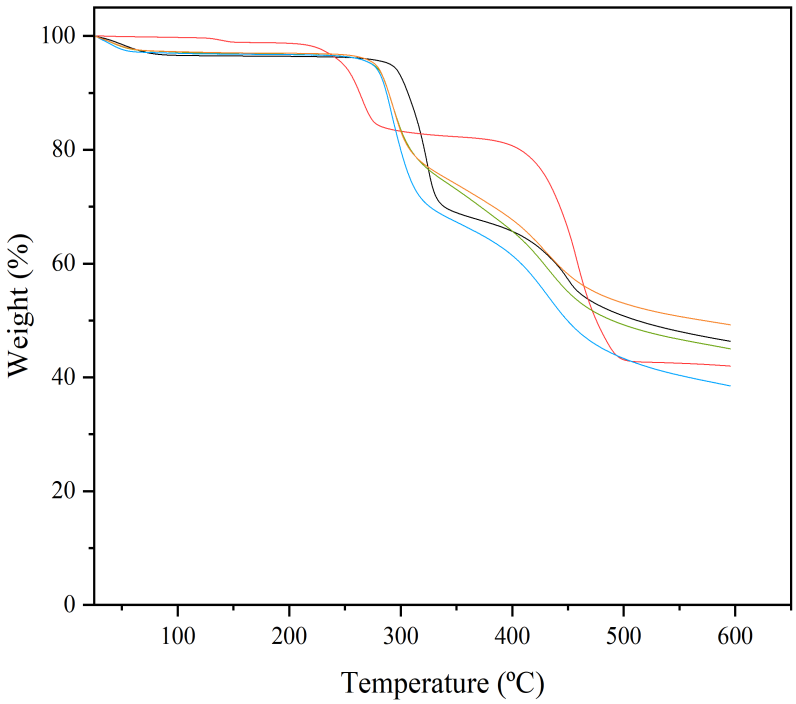

Figure 3. 11. Weight loss as a function of temperature of PIL $C(CN)_3$/40 [C_2MIM][$C(CN)_3$] (black); MOF-5 (red); PIL $C(CN)_3$/40 [C_2MIM][$C(CN)_3$]/10 MOF-5 (green); PIL $C(CN)_3$/40 [C_2MIM][$C(CN)_3$]/20 MOF-5 (blue); PIL $C(CN)_3$/40 [C_2MIM][$C(CN)_3$]/30 MOF-5 (orange).

Despite the decrease in both T_{onset} and T_{dec}, the increase of MOF-5 loading (from 10 to 30 wt%) not significantly affected the thermal stability of the prepared MMMs. Therefore, and even after the addiction of a material having lower thermal stability, such as MOF-5, it can be concluded that the thermal properties of the prepared MMMs membranes were not significantly different from those of the PIL/IL membranes. In previous studies, similar results have been observed for MOF-based MMMs,[88,92] in particular for PIL/IL/MOF membranes, when MIL-53 (Al), $Cu_3(BTC)_2$ and ZIF-8 were incorporated into the PIL Tf_2N/40 [Pyr_{11}][Tf_2N].[65] Overall, and considering that the temperature of biogas streams ranges between 25 and 35 ºC, it can be concluded that the prepared membranes fit in terms of thermal stability to be used for the biogas upgrading process.

3.2.2.5. Mechanical properties

In this work, the pucture test (described in section 2.2.2.7) allowed to determine the tensile strength and alongation of the prepared membranes. The aim was to verify the influence of MOF-5 incorporation on the mechanical properties of PIL/IL membranes. Throught **Equation 6** and **Equation 7** the tensile strength necessary to puncture the membranes and the alongation were calculated.

The results obtained for the PIL/IL membranes and respective PIL/IL/MOF-5 mixed matrix membranes are summarized in **Table 3.8** and **Table 3.9**.

The results showed in **Table 3.8** for the PIL Tf_2N/40 [C_2MIM][BETi]/MOF-5 membranes demonstrate lower values of tensile strength than that of the PIL Tf_2N/40 [C_2MIM][BETi]. The tensile strength decreases from 0.41 MPa for the former PIL/IL membrane to 0.18 MPa for the PIL/IL/MOF-5 mixed matrix membrane with the highest MOF-5 loading (30 wt%) and therefore, the tensile strength decreases as increasing MOF-5 concentration. Membranes alongation were also affect by MOF-5 incorporation, which slightly decrease with MOF-5 incorporation.

The PIL $C(CN)_3$/40 [C_2MIM][$C(CN)_3$] membrane presented a tensile strength of 0.46 ± 0.16 MPa (**Table 3.9**). With the addiction of MOF-5 in the membrane metrix, the tensile strength of the prepared membranes decreased as well as alongation. Comparing the three MMMs prepared, the increase of MOF-5 loading increase the tensile strength from 0.15 (10 wt%) to 0.30 MPa (30 wt%). The reduction of tensile strength and alongation results can be related with MOF-5 particles agglomerates in MMMs matrix, identified in SEM images (see section 3.2.2.1).

Table 3. 8. Puncture test results of PIL Tf_2N/40 [C_2MIM][BETi]/MOF-5 membranes

wt% MOF-5	Thickness (μm)	Tensile strength (MPa)	Alongation (%)
0	209 ± 7.97	0.41 ± 0.03	10.85 ± 1.70
10	48 ± 4.37	0.22 ± 0.13	9.05 ± 0.92
20	78 ± 7.57	0.21 ± 0.01	9.79 ± 0.57
30	57 ± 6.43	0.18 ± 0.00	8.60 ± 0.34

Table 3. 9. Puncture test results of PIL $C(CN)_3$/40 [C_2MIM][$C(CN)_3$]/MOF-5 membranes

wt% MOF-5	Thickness (μm)	Tensile strength (MPa)	Alongation (%)
0	134 ± 6.2	0.46 ± 0.16	6.14 ± 1.06
10	128 ± 8.7	0.15 ± 0.01	1.95 ± 0.20
20	100 ± 7.5	0.23 ± 0.04	3.83 ± 1.23
30	184 ± 7.4	0.30 ± 0.02	2.63 ± 0.48

Throught these results can be concluded that the addiction of MOF-5 particles probably decrease the free volume available of the prepared membrane, decrease the polymer chain mobility and, consequently, the membrane structure becomes more rigid and fragile. These behaviour was also reported in previous studies for other MOF-based MMMs.[65,92]

3.2.2.6. Gas permeation experiments

In this work, since the objective was the development of MMMs for CH_4 separation from biogas, gas permeability experiments were carried out for the gases present in higher quantity in biogas, namely, CO_2 and CH_4.

Initially, all the prepared PIL/IL membranes were tested in order to conclude which one had the best performance for CO_2/CH_4 separation. In order to evaluate the overall performance of the prepared membranes, the well-known Robeson upper bound limit was used, where the CO_2/CH_4 ideal selectivity is represented as a function of the CO_2 pure gas permeability. Therefore was possible to compare the obtained results with those available in the literature. The results are represented in **Figure 3.12**.

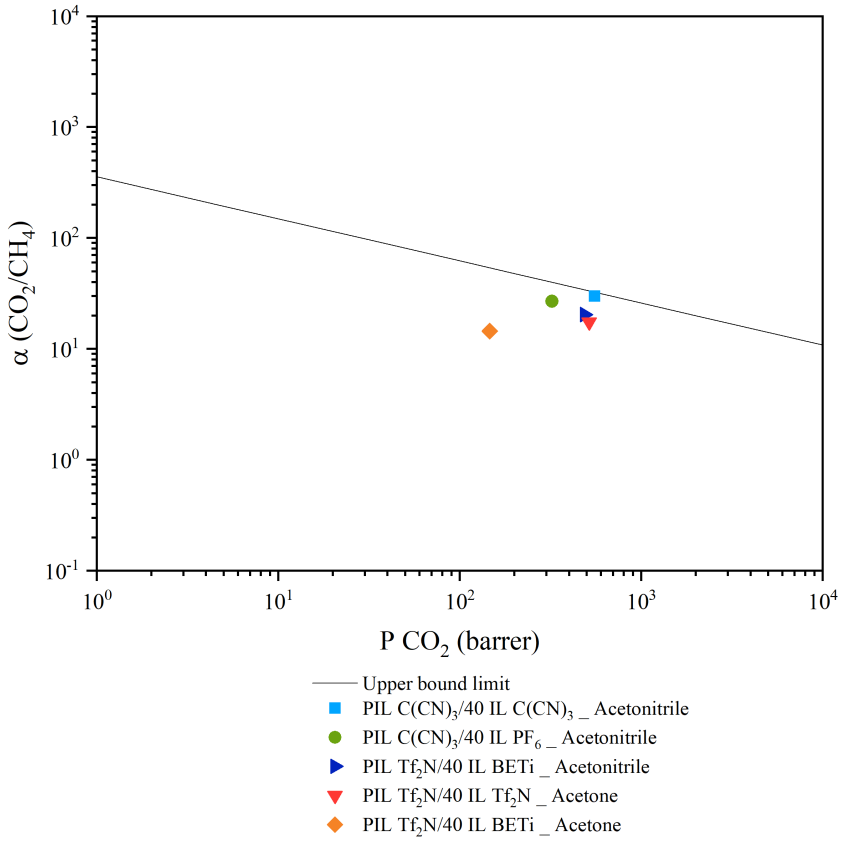

Figure 3. 12. CO_2/CH_4 PIL/IL ideal selectivity as a function of CO_2 permeability. Data are plotted on a log-log scale and the upper bound is adapted from Robeson.[54]

It is possible to observe that all the values are below the Robeson upper bound, which means that any of the prepared PIL/IL membranes achieve an ideal relation between the CO2 permeability and CO_2/CH_4 ideal selectivity. The membranes chosen were PIL $C(CN)_3$/40 $[C_2MIM][C(CN)_3]$_acetonitrile membrane and PIL Tf_2N/40 $[C_2MIM][BETi]$_acetone.

After choosing the best performance PIL/IL membranes, three different loadings of MOF-5 (10, 20 and 30 wt%) were incorporated into membrane matrix. At this time was conclude that MOF-5 did not dissolve in acetonitrile and therefore, was dicided to user another solvent, keeping the PIL/IL

composite membrane. Nevertheless, these membrane was not test in permeation experiments (see section 3.2.2).

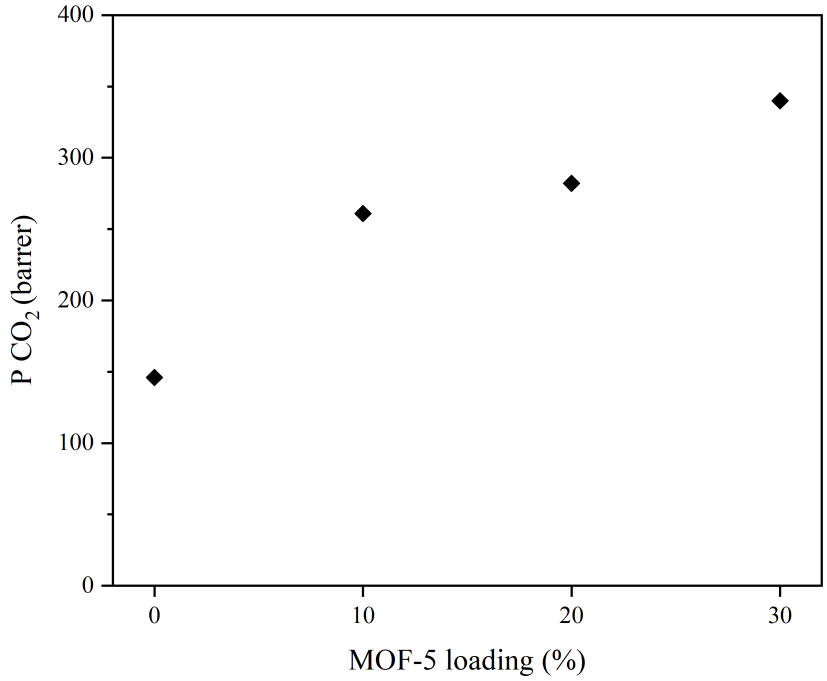

Figure 3. 13. Evolution of CO_2 of PIL Tf_2N/40 [C_2MIM][BETi] membranes permeability as a function of MOF-5 loading.

The results of the CO_2 single gas permeabilities of the prepared PIL Tf_2N/40 [C_2MIM][BETi] and the respectives MMMs, as a function of the MOF-5 loading, are illustrated in **Figure 3.13**. According to these results, as the MOF-5 concentration increases, CO_2 permeability also increases, from 146 barrer for the PIL/IL membrane to 340 barrer for the PIL/IL/MOF-5 membrane with 30 wt% loading. These behaviour is due to a greater diffusion of the gas molecules across the membrane, since the incorporation of MOF-5 particles provides an extra porous network for gas transport.[77] These results can also be translated in a good interaction between MOF-5 particles and the PIL/IL matrix.

Figure 3.14 displays the PIL/IL and PIL/IL/MOF-5 membranes performance through Robeson upper bound limit. It can be observed that, despite incorporating MOF-5 into PIL/IL matrix all experimental points bellow the upper bound limit. However, is possible to identify an increase in the CO_2 permeability for the MMMs, when compared to the PIL/IL membrane. The incorporation of MOF-5 also influences selectivity, which decreased as MOF-5 concentration increased, except for the MMM with 20 wt% of MOF-5 that was similar to the PIL/IL membrane. This fact can be explained based on MOF-5 porosity, which can induce an increase of diffusivity and the fact that its pore size (around 6 Å) is higher than the kinetic diameter of CO_2 and CH_4 (3.3 Å and 3.8 Å, respectively).[93] Despite that, can be concluded that CO_2 transport across the membrane is favoured over CH_4, since CO_2 solubility in

MOF-5 is higher than that of CH_4.[55] For comparison purposes **Table 3.10** displays literature values reported for other MMMs. It is clear that depending on the selection and loading degree of the different components present in the MMM (PIL, IL and MOF), different values of CO_2 permeability and CO_2/CH_4 selectivity can be achieved.

Table 3. 10. Selectivity and permeability of MMMs reported in the literature.

Mixed matrix membrane	α_{CO_2/CH_4}	P CO_2	Ref.
Poly[SMIM][Tf_2N]/20 [C_2MIM][Tf_2N]/20 SAPO-24	30	50	[94]
Poly[SMIM][Tf_2N]/20 [C_2MIM][Tf_2N]/20 SSZ-13	63	170	[94]
Poly[vbim][Tf_2N]/20 [C_2MIM][BF4]/20 ZIF-8	16.4	241	[95]
PI/33 [C_4mim][Tf_2N]/15 ZSM-15	24.1	34.4	[96]

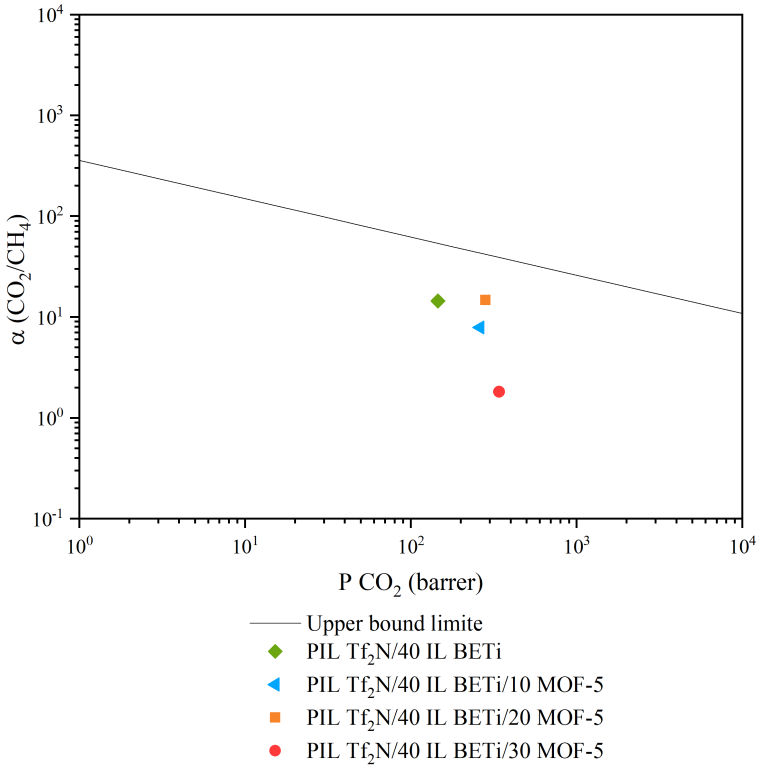

Figure 3. 14. CO_2/CH_4 MMMs ideal selectivity as a function of CO_2 permeability. Data are plotted on a log-log scale and the upper bound is adapted from Robeson.[54]

4. Conclusions

The aim of this thesis was the biogas production using a co-digestion system to treat saline effluents, namely a mixture of tannery and leachate, and, posteriorly, their purification using a membrane process based on mixed matrix membranes (MMMs) with the incorporation of MOF-5.

Concerning the first part, the effect of salinity on the system performance was assessed in this study. The single-stage co-digestion system strategy proved to be successful since a gradual adaptation of microbial culture to different salinities was observed, obtaining a high convertion of organic acids (OA), between 71.6 and 97.7 % and biogas production, between 1.6 ± 0.3 and 3.0 ± 0.3 L d^{-1} . Despite the disintegration of granules at 15 g Na^+ L^{-1}, the obtained results have demonstrated the feasibility of using anaerobic granules for the co-treatment of tanney and leachate up to 10 g Na^+ L^{-1}, which can produce biogas with 76.0 and 76.7% of CH_4.

In the second part, the synthetised MOF-5 was incorporated in two different PIL/IL combinations, namely PIL Tf_2N/40 [C_2MIM][BETi] using acetone as solvent and PIL $C(CN)_3$/40 [C_2MIM][$C(CN)_3$] using DMF. The influence of incorporating MOF-5 loadings on membrane morphology, thermal and mechanical stability, hydrophilic nature, as well as on the CO_2/CH_4 separation performance of the formed PIL/IL/MOF-5 membranes were evaluated.

The FTIR study confirmed the successful incorporation of [C_2MIM][BETi] IL and [C_2MIM][$C(CN)_3$] IL and MOF-5 within the [pyr_{11}][Tf_2N] PIL and [pyr_{11}][$C(CN)_3$] PIL matrices, respectively.

The SEM images of the PIL Tf_2N/40 [C_2MIM][BETi] membrane surface and cross-section revealed that dense, homogenous and defect-free membrane structure which indicates a good interaction between the polymer and the MOF-5. Relatively to PIL $C(CN)_3$/40 [C_2MIM][$C(CN)_3$] membrane, the appearance of some MOF-5 agglomerates in cross-section may indicate a poor interaction between the filler and the polymeric matrix. Nevertheless, the membrane presented a dense structure.

Through TGA analysis was possible to verify that, despite the lower thermal stability of MOF-5, the onset (< 383 ºC) and decomposition (< 412 ºC) temperatures of PIL Tf_2N/40 [C_2MIM][BETi] and the onset (< 279 ºC) and decomposition (< 573 ºC) temperatures of PIL $C(CN)_3$/40 [C_2MIM[$C(CN)_3$] were not significantly different compared to those of PIL/IL membranes and, thus, the prepared MMMs are suitable to biogas upgrading.

From the pucture tests, it was observed that the addiction of MOF-5 particles in the polymeric matrix decrease the tensile strength of the MMMs, originated more rigid and fragile membranes in comparison with the PIL/IL membranes. On the other hand, the results of contact angles measurements showed that the hydrophilic character remained the same with the incorporation of MOF, which is a quite important for CO_2 transport.

The pure gas permeation results showed that CO_2 permeability increased with the amount of MOF-

5 incorporated. The MMM with 30 wt% of MOF-5 achieved the highest CO_2 permeability of 340 Barrer. The only observed drawback was that the incorporation of MOF-5 resulted in a noticiable decrease in CO_2/CH_4 selectivity, possibly explained by the cavity size of MOF-5. However, it should be possible to improve the CO_2/CH_4 separation performance of this MMMs system by adjusting the amount of IL, or using different PILs, free ILs and MOF particles with higher CO_2/CH_4 selectivity. Althought further research is needed to achieve PIL/IL/MOF with better performance properties, the results of this thesis opens up the relevance of understanding at a molecular level the role of each component, in order to better tune-design MMMs for biogas upgrading.

5. Future work

From all the results obtained in this thesis relatively to both biogas production using a single-stage anaerobic digestion process and biogas purification using mixed matrix membranes with MOF-5, some suggestions to improve this study and possible for future work are presented:

1. Improve the adaptation of microbial culture to salinity, through a slower increase of sodium concentration.
2. Supplementation with calcium or iron can be a strategy to prevent granules disintegration since the integrity of granules can be controller by these nutrients.
3. Carry out gas permeation studies on the membranes using binary mixtures, namely CO_2/CH_4 that mimic the composition, temperature and pressure of the biogas stream.
4. Adjusting the amount of IL, or using different PILs, free ILs and MOF particles with higher CO_2/CH_4 selectivity.
5. Use another solvents to prepare the PIL $C(CN)_3$/40 $[C_2MIM][C(CN)_3]$ membrane.

6. References

1. Nasir IM, Ghazi TIM, Omar R. Production of biogas from solid organic wastes through anaerobic digestion : a review. *Springer*. 2012:321-329. doi:10.1007/s00253-012-4152-7
2. Li Y, Park SY, Zhu J. Solid-state anaerobic digestion for methane production from organic waste. *Renew Sustain Energy Rev*. 2011;15:821-826. doi:10.1016/j.rser.2010.07.042
3. Danthurebandara M, Passel S Van, Nelen D, Tielemans Y, Machiels G, Use L. Environmental and socio-economic impacts of landfills. 2013;(January).
4. Lefebvre O, Moletta R. Treatment of organic pollution in industrial saline wastewater: A literature review. *Water Res*. 2006;40(20):3671-3682. doi:10.1016/J.WATRES.2006.08.027
5. Zhang C, Su H, Baeyens J, Tan T. Reviewing the anaerobic digestion of food waste for biogas production. *Renew Sustain Energy Rev*. 2014;38:383-392. doi:10.1016/J.RSER.2014.05.038
6. Youcai Z, Youcai Z. Leachate Generation and Characteristics. *Pollut Control Technol Leachate from Munic Solid Waste*. January 2018:1-30. doi:10.1016/B978-0-12-815813-5.00001-2
7. Ghosh S, Hasan S. Anaerobic digestion of landfill leachate : A modified approach. 2015;(July 2013).
8. Ali M, Elreedy A, Tawfik A. Feasibility of Using Hypersaline Lake Sediment as Inoculum for Biogas Production from Anaerobic Digestion of Saline Wastewater. 2018;(April):153-156. doi:10.1145/3180382.3180410
9. Buljan J, Kral I. Introduction To Treatment of Tannery Effluents. *United Nations Ind Dev Organ*. 2011:1-69.
10. *Waste Water Report 2018 - The Reuse Opportunity*. London, UK; 2018. doi:10.5194/acp-2016-176
11. Puyol D, Batstone DJ, Hülsen T, Astals S, Peces M, Krömer JO. Resource recovery from wastewater by biological technologies: Opportunities, challenges, and prospects. *Front Microbiol*. 2017;7(JAN). doi:10.3389/fmicb.2016.02106
12. Fauziah SH, Emenike CU, Agamuthu P. Leachate risk and identification of accumulated heavy metals in Pangasius sutchi. *Waste Manag Res*. 2013;31(10 SUPPL.):75-80. doi:10.1177/0734242X13492840
13. Weiland P. Biogas production : current state and perspectives. *Springer*. 2010:849-860. doi:10.1007/s00253-009-2246-7
14. Kangle, K. M.; Kore, S. V.; Kore, V. S.; Kulkarni GS. Recent Trends in Anaerobic Codigestion : A Review. *Univers J Environ Res Technol*. 2012;2(4):210-219. http://www.environmentaljournal.org/2-4/ujert-2-4-3.pdf.
15. Lier JB Van, Mahmoud N, Zeeman G. *Anaerobic Wastewater Treatment*.; 2008.
16. Abbasi T, Tauseef SM, Abbasi SA. Anaerobic digestion for global warming control and energy

generation — An overview. *Renew Sustain Energy Rev*. 2012;16(5):3228-3242. doi:10.1016/j.rser.2012.02.046

17. Bothi KL. Characterization of Biogas From Anaerobically Digested Dairy Waste For Energy Use. 2007;(May).
18. Costa A, Ely C, Pennington M, Rock S, Staniec C, Turgeon J. Anaerobic Digestion and its Applications. *United States Environ Prot Agency*. 2015;(October):15.
19. Bajpai P. Basics of Anaerobic Digestion Process. *Springer*. 2017:7-13. doi:10.1007/978-981-10-4130-3
20. N. Meegoda J, Li B, Patel K, B. Wang L. A Review of the Processes, Parameters, and Optimization of Anaerobic Digestion. *Int J Environ Res Public Health*. 2018. doi:10.3390/ijerph15102224
21. Amani T, Nosrati M, Sreekrishnan TR. Anaerobic digestion from the viewpoint of microbiological , chemical , and operational aspects — a review. 2010;278:255-278. doi:10.1139/A10-011
22. Zupan GD, Grilc V. Anaerobic Treatment and Biogas Production from Organic Waste. 2007;2.
23. Alvarado LR. Optimization of the electron donor supply to sulphate reducing bioreactors treating inorganic wastewater. 2018.
24. Begum S, Rao G, Sridhar S, Bhargava SK, Jegatheesan V, Eshtiaghi N. Evaluation of single and two stage anaerobic digestion of landfill leachate : Effect of pH and initial organic loading rate on volatile fatty acid (VFA) and biogas production. 2018;251(November 2017):364-373. doi:10.1016/j.biortech.2017.12.069
25. Voelklein MA, Jacob A, Shea RO, Murphy JD. Assessment of increasing loading rate on two-stage digestion of food waste. *Bioresour Technol*. 2016;202:172-180. doi:10.1016/j.biortech.2015.12.001
26. Chowdhury P, Viraraghavan T, Srinivasan A. Bioresource Technology Biological treatment processes for fish processing wastewater – A review. *Bioresour Technol*. 2010;101(2):439-449. doi:10.1016/j.biortech.2009.08.065
27. Demirel B, Yenigun O. Two-phase anaerobic digestion processes : a review. *J Chem Technol Biotechnol*. 2002;755(January):743-755. doi:10.1002/jctb.630
28. De Mes TZD, Stams AJM, Reith JH, Zeeman G. Methane production by anaerobic digestion of wastewater and solid wastes. In: Reith JH, Wijffels RH, Barten H, eds. *Bio-Methane & Bio-Hydrogen*. ; 2003:58-102.
29. Alphenaar A. Anaerobic granular sludge: Characterization, and factors affecting its functioning. 1995.
30. Dewil R, Appels L, Baeyens J, Degre J. Principles and potential of the anaerobic digestion of waste-activated sludge. *Prog Energy Combust Sci*. 2008;34:755-781. doi:10.1016/j.pecs.2008.06.002

31. Chen L, Neibling H. *Anaerobic Digestion Basics*.; 2014.
32. Sudmalis D, Gagliano MC, Pei R, et al. Fast anaerobic sludge granulation at elevated salinity. *Water Res*. 2018;128:293-303. doi:10.1016/j.watres.2017.10.038
33. Abdelgadir A, Chen X, Liu J, et al. Characteristics, process parameters, and inner components of anaerobic bioreactors. *Biomed Res Int*. 2014;2014. doi:10.1155/2014/841573
34. Paudel S, Kang Y, Yoo Y, Tae G. Effect of volumetric organic loading rate (OLR) on H 2 and CH 4 production by two-stage anaerobic co-digestion of food waste and brown water. *Waste Manag*. 2017;61:484-493. doi:10.1016/j.wasman.2016.12.013
35. Mao C, Feng Y, Wang X, Ren G. Review on research achievements of biogas from anaerobic digestion. *Renew Sustain Energy Rev*. 2015;45:540-555. doi:10.1016/j.rser.2015.02.032
36. Sibiya NT, Tesfagiorgis HB, Muzenda E. Influence of Nutrients Addiction for Enhanced Biogas Production from Energy Crops: A Review. In: ; 2015:132-135. doi:http://dx.doi.org/10.15242/IIE.E1115038
37. Awe OW, Zhao Y, Nzihou A, et al. A Review of Biogas Utilisation , Purification and Upgrading Technologies. 2018.
38. Petersson A, Wellinger A. *Biogas Upgrading Technologies-Developments and Innovations*.; 2011. www.iea-biogas.net.
39. Ullah Khan I, Hafiz Dzarfan Othman M, Hashim H, et al. Biogas as a renewable energy fuel – A review of biogas upgrading, utilisation and storage. *Energy Convers Manag*. 2017;150(July):277-294. doi:10.1016/j.enconman.2017.08.035
40. Niesner J, Jecha D, Stehlík P. Biogas upgrading technologies: State of art review in european region. *Chem Eng Trans*. 2013;35(January):517-522. doi:10.3303/CET1335086
41. Technische Universität Wien. Biogas To Biomethane Technology Review. *Vienna Univ Technol*. 2012;(May):1-15. http://bio.methan.at/sites/default/files/BiogasUpgradingTechnologyReview_ENGLISH.pdf.
42. Ramdin M, Loos TW De, Vlugt TJH. *State-of-the-Art of CO2 Capture with Ionic Liquids*.; 2012. doi:10.1021/ie3003705
43. *Three Basic Methods to Separate Gases*.; 2008. doi:http://www.co2captureproject.org/pdfs/3_basic_methods_gas_separation.pdf
44. Scholz M, Melin T, Wessling M. Transforming biogas into biomethane using membrane technology. *Renew Sustain Energy Rev*. 2013;17:199-212. doi:10.1016/j.rser.2012.08.009
45. Lestinsky P, Vecer M, Navrátil P, Stehlík P. Removing CO_2 from Biogas – the Optimisation of a Pressure Swing Adsorption (PSA) Unit Using Breakthrough Curves. *Chem Eng Trans*. 2014;39(August):265-270. doi:10.3303/CET1439045
46. Andriani D, Wresta A, Atmaja TD, Saepudin A. A review on optimization production and upgrading biogas through CO2removal using various techniques. *Appl Biochem Biotechnol*. 2014;172(4):1909-1928. doi:10.1007/s12010-013-0652-x

47. Augelletti R, Conti M, Annesini MC. Pressure swing adsorption for biogas upgrading. A new process configuration for the separation of biomethane and carbon dioxide. *J Clean Prod*. 2017;140:1390-1398. doi:10.1016/J.JCLEPRO.2016.10.013
48. Mulder M. *Basic Principles of Membrane Technology*. Second Edi. Kluwer Academic Publishers; 2003.
49. Makaruk A, Miltner M, Harasek M. Membrane biogas upgrading processes for the production of natural gas substitute. *Sep Purif Technol*. 2010;74(1):83-92. doi:10.1016/j.seppur.2010.05.010
50. Brunetti A, Scura F, Barbieri G, Drioli E. Membrane technologies for CO2 separation. *J Memb Sci*. 2010;359(1-2):115-125. doi:10.1016/j.memsci.2009.11.040
51. Vrbová V, Ciahotný K. Upgrading Biogas to Biomethane Using Membrane Separation. *Energy and Fuels*. 2017;31(9):9393-9401. doi:10.1021/acs.energyfuels.7b00120
52. Chung TS, Jiang LY, Li Y, Kulprathipanja S. Mixed matrix membranes (MMMs) comprising organic polymers with dispersed inorganic fillers for gas separation. *Prog Polym Sci*. 2007;32(4):483-507. doi:10.1016/j.progpolymsci.2007.01.008
53. Jeazet HBTJ, Staudt C, Janiak C. Metal-Organic frameworks in mixed-matrix membranes for gas separation. *Dalt Trans*. 2012;41(46):14003-14027. doi:10.1039/c2dt31550e
54. Robeson LM. The upper bound revisited. 2008;320:390-400. doi:10.1016/j.memsci.2008.04.030
55. Arjmandi M, Pakizeh M. Mixed matrix membranes incorporated with cubic-MOF-5 for improved polyetherimide gas separation membranes : Theory and experiment. *J Ind Eng Chem*. 2014;20(5):3857-3868. doi:10.1016/j.jiec.2013.12.091
56. Panapitiya N, Wijenayake S, Nguyen D, et al. Compatibilized immiscible polymer blends for gas separations. *Materials (Basel)*. 2016;9(8). doi:10.3390/ma9080643
57. Aroon MA, Ismail AF, Matsuura T, Montazer-Rahmati MM. Performance studies of mixed matrix membranes for gas separation: A review. *Sep Purif Technol*. 2010;75(3):229-242. doi:10.1016/j.seppur.2010.08.023
58. Rosyadah Ahmad NN, Mukhtar H, Mohshim DF, Nasir R, Man Z. Surface modification in inorganic filler of mixed matrix membrane for enhancing the gas separation performance. *Rev Chem Eng*. 2016;32(2):181-200. doi:10.1515/revce-2015-0031
59. Cheng Y, Ying Y, Zhai L, et al. Mixed matrix membranes containing MOF@COF hybrid fillers for efficient CO 2 /CH 4 separation. *J Memb Sci*. 2019;573(November 2018):97-106. doi:10.1016/j.memsci.2018.11.060
60. Mecerreyes D. Polymeric ionic liquids: Broadening the properties and applications of polyelectrolytes. *Prog Polym Sci*. 2011;36(12):1629-1648. doi:10.1016/j.progpolymsci.2011.05.007
61. L.C.Tomé. Development of new membranes based on ionic liquid materials for gas separation. 2014.

62. Fujie K, Kitagawa H. Ionic liquid transported into metal-organic frameworks. *Coord Chem Rev*. 2016;307:382-390. doi:10.1016/j.ccr.2015.09.003
63. Tomé LC, Florindo C, Freire CSR, Rebelo LPN, Marrucho IM. Playing with ionic liquid mixtures to design engineered CO2 separation membranes. *Phys Chem Chem Phys*. 2014;16(32):17172-17182. doi:10.1039/c4cp01434k
64. Tomé LC, Guerreiro DC, Teodoro RM, Alves VD, Marrucho IM. Effect of polymer molecular weight on the physical properties and CO 2 /N 2 separation of pyrrolidinium-based poly(ionic liquid) membranes. *J Memb Sci*. 2018;549(December 2017):267-274. doi:10.1016/j.memsci.2017.12.019
65. Nabais AR, Martins APS, Alves VD, et al. Poly(ionic liquid)-based engineered mixed matrix membranes for CO2/H2 separation. *Sep Purif Technol*. 2019. doi:10.1016/j.seppur.2019.04.018
66. Adatoz E, Avci AK, Keskin S. Opportunities and challenges of MOF-based membranes in gas separations. *Sep Purif Technol*. 2015;152:207-237. doi:10.1016/j.seppur.2015.08.020
67. Li JR, Ma Y, McCarthy MC, et al. Carbon dioxide capture-related gas adsorption and separation in metal-organic frameworks. *Coord Chem Rev*. 2011;255(15-16):1791-1823. doi:10.1016/j.ccr.2011.02.012
68. Li H, Eddaoudi M, O'Keeffe M, Yaghi OM. Design and synthesis of an exceptionally stable and highly porous metal-organic framework. *Nature*. 1999;402(November):276-279.
69. Lowry OH, Rosebrough NJ, Farr AL, Randall RJ. Protein measurement with the folin phenol reagent. 1951:265-275.
70. APHA/AWWA. *Standard Methods for the Examination of Water and Wastewater*. Port City. Baltimore; 1995.
71. Tomé LC, Isik M, Freire CSR, Mecerreyes D, Marrucho IM. Novel pyrrolidinium-based polymeric ionic liquids with cyano counter-anions: HIGH performance membrane materials for post-combustion CO2 separation. *J Memb Sci*. 2015. doi:10.1016/j.memsci.2015.02.020
72. Sabouni R, Kazemian H, Rohani S. A novel combined manufacturing technique for rapid production of IRMOF-1 using ultrasound and microwave energies. *Chem Eng J*. 2010;165(3):966-973. doi:10.1016/j.cej.2010.09.036
73. Ata-ur-Rehman, Tirmizi SA, Badshah A, et al. Synthesis of highly stable MOF-5@MWCNTs nanocomposite with improved hydrophobic properties. *Arab J Chem*. 2018;11(1):26-33. doi:10.1016/j.arabjc.2017.01.012
74. Saha D, Bao Z, Jia F, Deng S. Adsorption of CO2,CH4,N2O, and N2 on MOF-5, MOF-177, and Zeolite 5A. *Environ Sci Technol*. 2010;44:1820-1826.
75. Greathouse JA, Allendorf MD. The interaction of water with MOF-5 simulated by molecular dynamics. *J Am Chem Soc*. 2006;128(33):10678-10679. doi:10.1021/ja063506b
76. AYKAÇ ÖZEN H, ÖZTÜRK B, ÖBEKCAN H. Synthesis, Characterization and Gas Separation Properties of MOF-5 Mixed Matrix Membranes. *Nevşehir Bilim ve Teknol Derg*. 2017;6:415-

423. doi:10.17100/nevbiltek.332792

77. Perez E V., Balkus KJ, Ferraris JP, Musselman IH. Mixed-matrix membranes containing MOF-5 for gas separations. *J Memb Sci*. 2009;328(1-2):165-173. doi:10.1016/J.MEMSCI.2008.12.006

78. Zhao Z, Ma X, Kasik A, Li Z, Lin YS. Gas separation properties of metal organic framework (MOF-5) membranes. *Ind Eng Chem Res*. 2013;52(3):1102-1108. doi:10.1021/ie202777q

79. Ming Y, Purewal J, Liu D, et al. Thermophysical properties of MOF-5 powders. *Microporous Mesoporous Mater*. 2014;185:235-244. doi:10.1016/j.micromeso.2013.11.015

80. Neves LA, Crespo JG, Coelhoso IM. Gas permeation studies in supported ionic liquid membranes. *J Memb Sci*. 2010;357(1-2):160-170. doi:10.1016/j.memsci.2010.04.016

81. Capson-Tojo G, Ruiz D, Rouez M, et al. Accumulation of propionic acid during consecutive batch anaerobic digestion of commercial food waste. *Bioresour Technol*. 2017;245(August):724-733. doi:10.1016/j.biortech.2017.08.149

82. Li J, Ban Q, Zhang L, Jha AK. Syntrophic propionate degradation in anaerobic digestion: A review. *Int J Agric Biol*. 2012;14(5):843-850.

83. Parawira W, Murto M, Zvauya R, Mattiasson B. Comparative performance of a UASB reactor and an anaerobic packed-bed reactor when treating potato waste leachate. *Renew Energy*. 2006;31(6):893-903. doi:10.1016/j.renene.2005.05.013

84. Gebauer R. Mesophilic anaerobic treatment of sludge from saline fish farm effluents with biogas production. *Bioresour Technol*. 2004;93(2):155-167. doi:10.1016/j.biortech.2003.10.024

85. Bouallagui H, Torrijos M, Godon JJ, et al. Two-phases anaerobic digestion of fruit and vegetable wastes: Bioreactors performance. *Biochem Eng J*. 2004;21(2):193-197. doi:10.1016/j.bej.2004.05.001

86. Xiao Y, Roberts DJ. A review of anaerobic treatment of saline wastewater. *Environ Technol*. 2010;31(8-9):1025-1043. doi:10.1080/09593331003734202

87. Chen B, Wang X, Zhang Q, et al. Synthesis and characterization of the interpenetrated MOF-5 †. 2010:3758-3767. doi:10.1039/b922528e

88. Monteiro B, Nabais AR, Almeida Paz FA, et al. Membranes with a low loading of Metal–Organic Framework-Supported Ionic Liquids for CO2/N2 separation in CO2 capture. *Energy Technol*. 2017;5(12):2158-2162. doi:10.1002/ente.201700228

89. Bakhtiari O, Sadeghi N. The Formed Voids around the Filler Particles Impact on the Mixed Matrix Membranes' Gas Permeabilities. *Int J Chem Eng Appl*. 2014;5(2):198-203. doi:10.7763/ijcea.2014.v5.378

90. Tomé LC, Aboudzadeh MA, Rebelo LPN, Freire CSR, Mecerreyes D, Marrucho IM. Polymeric ionic liquids with mixtures of counter-anions: A new straightforward strategy for designing pyrrolidinium-based CO2 separation membranes. *J Mater Chem A*. 2013;1(35):10403-10411. doi:10.1039/c3ta12174g

91. Kiefer J, Noack K, Penna TC, Ribeiro MCC, Weber H, Kirchner B. Vibrational signatures of

anionic cyano groups in imidazolium ionic liquids. *Vib Spectrosc*. 2017;91:141-146. doi:10.1016/j.vibspec.2016.05.004

92. Nabais AR, Ribeiro RPPL, Mota JPB, Alves VD, Esteves IAAC, Neves LA. CO2/N2 gas separation using Fe(BTC)-based mixed matrix membranes: A view on the adsorptive and filler properties of metal-organic frameworks. *Sep Purif Technol*. 2018;202(March):174-184. doi:10.1016/j.seppur.2018.03.028
93. Kentish S, Scholes C, Stevens G. Carbon Dioxide Separation through Polymeric Membrane Systems for Flue Gas Applications. *Recent Patents Chem Eng*. 2012;1(1):52-66. doi:10.2174/2211334710801010052
94. Singh Z V., Cowan MG, McDanel WM, et al. Determination and optimization of factors affecting CO2/CH4 separation performance in poly(ionic liquid)-ionic liquid-zeolite mixed-matrix membranes. *J Memb Sci*. 2016;509(February):149-155. doi:10.1016/j.memsci.2016.02.034
95. Hao L, Li P, Yang T, Chung TS. Room temperature ionic liquid/ZIF-8 mixed-matrix membranes for natural gas sweetening and post-combustion CO2 capture. *J Memb Sci*. 2013;436:221-231. doi:10.1016/j.memsci.2013.02.034
96. Shindo R, Kishida M, Sawa H, et al. Characterization and gas permeation properties of polyimide/ZSM-5 zeolite composite membranes containing ionic liquid. *J Memb Sci*. 2014;454:330-338. doi:10.1016/j.memsci.2013.12.031